Supplement to

Cornea

Volume 37

Number 6

June 2018

Contents

Supplement Articles

(continued next page)

Wolters Kluwer

Cornea, The Journal of Cornea and External Disease (ISSN: #0277-3740) is published monthly by Wolters Kluwer Health, Inc., at 14700 Citicorp Drive, Bldg 3, Hagerstown, MD 21742. Business and production offices are located at Two Commerce Square, 2001 Market St., Philadelphia, PA 19103. Periodicals postage paid at Hagerstown, MD and at additional mailing offices.

Annual subscription rates: $823 Individual Domestic, $2157 Institutional Domestic, $357 In-training Domestic; $896 Individual International, $2228 Institutional International, $357 In-training International. Single copy rate $171.00. Handling fee is $18. Subscriptions outside of North America must add $20.00 for airfreight delivery. United States residents of AL, CO, DC, FL, GA, HI, IA, ID, IN, KS, KY, LA, MD, MO, ND, NM, NV, PR, RI, SC, SD, UT, VT, WA, WV add state sales tax. The GST tax of 7% must be added to all orders shipped to Canada (Wolters Kluwer Health's GST Identification #895524239, Publications Mail Agreement #1119672). Subscription prices outside the United States must be prepaid. Prices subject to change without notice. Prices include shipping and handling. Visit us online at www.lww.com.

POSTMASTER: Send address changes to *Cornea*, The Journal of Cornea and External Disease, PO Box 1610, Hagerstown, MD 21740.

Contents *(continued)*

Acknowledgment for Support

The coeditors and contributors are most appreciative of the financial support for staff time and funds for the following eye banks:

Cleveland Eye Bank Foundation
Eversight
Indiana Lions Eye Bank
Iowa Lions Eye Bank
Keralink
Lions VisionGift
OneLegacy
Rocky Mountain Lions Eye Bank
SightLife

Visit the Journal's website at:
www.corneajrnl.com

Instructions for Authors can be found on the journal's website in the Author and Reviewer Information section. All manuscripts must be submitted on-line through the Cornea Web site at: https://cornea.edmgr.com.

The Cornea Journal
4000 Legato Rd
Ste 700
Fairfax, VA 22033
Telephone: 703.591.2220
Facsimile: 703.547.8861
e-mail: lburke@corneasociety.org

Listed in *Index Medicus/MEDLINE, Current Contents/Clinical Medicine, Scisearch, Excerpta Medica, Ocular Resources Review,* and *Ophthalmic Literature.*

Article and issue photocopies and 16-mm microfilm, 35-mm microfilm, and 105-mm microfiche are available from UMI, 300 North Zeeb Road, Ann Arbor, MI 48106-1346.

Address for non-member subscription information, orders, or change of address: Wolters Kluwer Health, 14700 Citicorp Drive, Bldg 3, Hagerstown, MD 21742; phone 800-638-3030; fax 301-223-2400. In Japan, contact Wolters Kluwer Health Japan Co., Ltd., Forecast Mita Building 5th floor, 1-3-31 Mita Minato-ku, Tokyo, Japan 108-0073. Telephone: +81 3 5427 1969. E-mail: journal@wkjapan.co.jp

Printed in the United States of America.

Current and New Technologies in Corneal Donor Tissue Evaluation: Comparative Image Atlas

Coeditors:
Kayla E. Gray, CCRP
Innovations Operations Supervisor, Biorepository, Eversight

Beth Ann Benetz, CRA, FOPS
Professor, Department of Ophthalmology and Visual Sciences,
Case Western Reserve University,
Scientific Director, CIARC and REDIARC

Christopher G. Stoeger, MBA, CEBT
Chief Executive Officer, Lions VisionGift

Jonathan H. Lass, MD
Charles I Thomas Professor, Case Western Reserve University,
Department of Ophthalmology and Visual Sciences,
Medical Director, Eversight
Medical Director, CIARC and REDIARC

Received for publication February 28, 2018; revision received March 6, 2018; accepted March 6, 2018.
Correspondence: Jonathan H. Lass, MD, University Hospitals Cleveland Medical Center, 11100 Euclid Avenue, Cleveland, OH 44106 (e-mail: jonathan.lass@uhhospitals.org).

Contributors
Participating Eye Banks and Individuals

Donor Network of Arizona
Anthony Vizzerra*
David Brandon Edwards
James Chavarria
Nate Stuart

Lions VisionGift
Jameson Clover*^
Daniel Davis
Amy Ansin*

Iowa Lions Eye Bank
Adam Stockman*^
Monica Freiburger*
Scott Van Oss
Greg Schmidt

SightLife
Mimi Chau
Esteban Peralta

Miracles in Sight
Sara Botsay*
Tyler Wrench
Holly Pegram

Lions Eye Bank of Eastern Virginia
Karen Kirkpatrick*
Brian Philippy
Kate Dorhout
Jacklyn Stone
Christina Robbins
Aaron Glore
Nicole Miller

Lions Gift of Sight
Jeff Justin
Peter Bedard
Veronique Grimes

OneLegacy
Gonzalo Lazarte

Rocky Mountain Lions Eye Bank
John Lohmeier*
Jason Christy

Eversight
Kayla Jones
Lindsey Savitt
Holly Hartman
Chemika Howard
Shalin Patel
Susan Hurlburt
Kristen McCoy
Marguerite Delvecchio
Gregory Grossman, PhD
Nicole Breimaier Rozsa

*Denotes section leader.
^Denotes introduction leader.

Introduction

Kayla E. Gray, CCRP, Beth Ann Benetz, CRA, FOPS, Christopher G. Stoeger, MBA, CEBT, and Jonathan H. Lass, MD

Eye banks are entrusted with a precious benevolent gift—the gift of donated human ocular tissues. Not only has the donor and donor family placed their trust in eye banks, trust runs deep in the corneal transplant community that eye banks will provide only the highest quality tissue for surgery. The donated tissue must be disease-free and have the capacity to function in the recipient for many years, while tissue screening must be completed in a precise and timely manner. Tissue screening is a delicate balance that, by design, requires eye banks to determine tissue suitability in situations that at times can be somewhat ambiguous. Ambiguity, by necessity, leads to erring on the side of safety and ruling tissue ineligible for transplantation, which in turns leads to the potential of waste of a donor's gift.

Modern technology has brought additional resources to the evaluation process to aid in tissue screening of the hypothermically stored donor cornea (Fig. 1). Slit-lamp examination has been the mainstay for tissue evaluation over the course of corneal transplantation since its advent in the 20th century. Specular microscopy was subsequently applied to eye banking tissue evaluation by Bourne and others in the 1970s[1] but did not become a requirement of the Eye Bank Association of America in Medical Standards until 2001.[2] Since that time, slit-lamp examination and specular microscopy have complemented each other in tissue assessment for suitability with slit-lamp examination ideal for assessment of the epithelium, stroma, folds, and lower power view of the endothelium, whereas specular microscopy provides a high power view of the endothelial mosaic enabling determination of density and abnormalities (eg, guttae). Since its introduction, optical coherence tomography has been used for its noncontact measuring capabilities related to endothelial keratoplasty (EK) graft thickness.[3–5] Ancillary screening benefits from this technology now aid those eye banks that use this technology for evaluation of disease processes of the epithelium and stroma (eg, infiltrate).[6,7] Finally, a fourth imaging tool is now available to aid tissue screening with the ex vivo wide-field dual imaging noncontact specular microscope (CellChek® D+®, Konan Medical, Irvine, CA) with its Enhanced mode and Finder mode views.

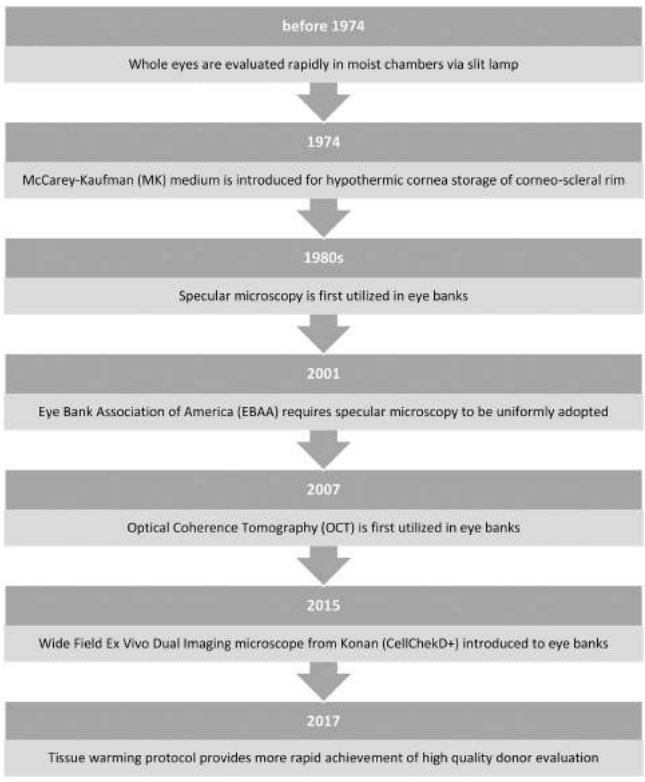

FIGURE 1. Timeline of the advancements in eye banking.

To our knowledge, this atlas provides for the first time reference images combining the use of all 4 technologies to provide a comprehensive approach to current donor cornea tissue evaluation with the hypothermically stored donor cornea. Because organ culture is not used in the United States, the coeditors elected to restrict this atlas to the hypothermically stored donor cornea but would welcome our organ culture colleagues to develop a similar atlas. Normal and diseased states of tissue are presented in a manner which will provide detailed resources for training of both new and experienced eye bank technicians. As our understanding of imaging technology advances, surgeons can have a greater assurance that only tissue appropriate for use has been released while at the same time stewardship over the donated gift is honored. Ultimately, surgeons are the final arbiter of suitability for their individual patients. This advancement will help provide the most accurate information possible regarding tissue suitability determinations among surgeons and eye bankers.

This atlas is a collaboration among 10 eye banks. More than 300 images of corneas were submitted over the course of 2 years. It is organized such that each layer of the cornea is given its own section. In addition, a separate section on tissue processed for EK has been established. And finally, a section devoted to findings that do not fit neatly into an anatomic category rounds out the atlas. This atlas been created for the field of eye banking to share information as a community

committed to providing the highest quality tissue possible for sight restoration.

REFERENCES

1. Bourne WM. Examination and Photography of donor corneal endothelium. *Arch Ophthalmol.* 1976;94:1799–1800.
2. Eye Bank Association of America. *Medical Standards*. Washington, DC: Eye Bank Association of America; 2017.
3. Tang M, Stoeger C, Galloway J, et al. Evaluating DSAEK graft deturgescence in preservation medium after microkeratome cut with optical coherence tomography. *Cornea.* 2013;32:847–850.
4. Brown JS, Wang D, Li X, et al. In situ ultrahigh-resolution optical coherence tomography characterization of eye bank corneal tissue processed for lamellar keratoplasty. *Cornea.* 2008;27:802–810.
5. Woodward MA, Titus MS, Shtein RM. Effect of microkeratome pass on tissue processing for Descemet stripping automated endothelial keratoplasty. *Cornea.* 2014;33:507–509.
6. Bald MR, Stoeger C, Galloway J, et al. Use of fourier-domain optical coherence tomography to evaluate anterior stromal opacities in donor corneas. *J Ophthalmol.* 2013;2013:397680.
7. Lin RC, Li Y, Tang M, et al. Screening for previous refractive surgery in eye bank corneas by using optical coherence tomography. *Cornea.* 2007; 26:594–599.

Slit-Lamp Biomicroscopy

Jameson Clover, CEBT

(*Cornea* 2018;37:S5–S6)

Slit-lamp biomicroscopy has been the hallmark of donor cornea evaluation since the beginning of retrieval of cadaveric whole eyes over the past century and subsequently corneal tissue in viewing chambers or vials over the past nearly 50 years. Tissue evaluation is a fundamental eye bank function and is required by the Eye Bank Association of America to determine surgical suitability. Slit-lamp biomicroscopy in turn has been a fundamental method of tissue evaluation since the Eye Bank Association of America instituted the criteria for eye bank and technician certification in 1980.[1] Subsequently, specular microscopy was added relatively recently as another essential method for evaluation of the endothelium in 2001.[2]

The slit-lamp biomicroscopy technique has not changed essentially in the past several decades. Although the technology has remained unchanged, except for improved optics, slit-lamp examination remains the gold standard for determining surgical suitability. This is in large part due to the dynamic nature of the slit lamp, which allows the evaluator to examine all layers of the cornea from both anterior and posterior perspectives, making it one of the most comprehensive techniques available to eye bankers.

Other modalities, such as specular microscopy and optical coherence tomography, primarily focus on a single corneal layer or cross section, whereas the slit lamp is used to evaluate all layers using different magnifications and illumination techniques to highlight different findings relative to the layer being evaluated (Fig. 1). A technician can easily go from observing the overall tissue with low magnification to

FIGURE 1. Slit-lamp biomicroscope.

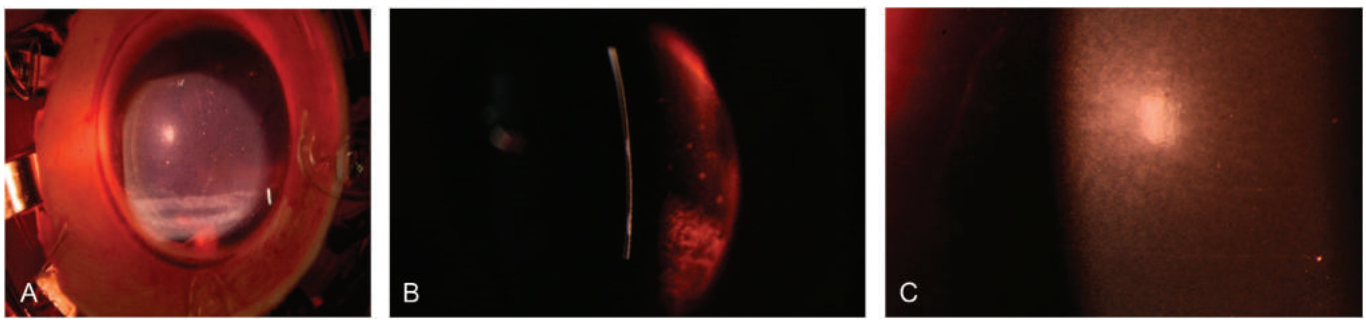

FIGURE 2. A, Low-magnification, diffuse view of overall tissue. B, Slit beam to sweep stroma; opacities are identified. C, Specular reflection of endothelial mosaic.

Received for publication February 28, 2018; revision received March 6, 2018; accepted March 6, 2018.

sweeping the cornea with a fine slit beam to identify possible stromal pathologies and then using high magnification to scrutinize the endothelium. The most common types of illumination include direct illumination, retroillumination, specular reflection, and sclerotic scatter (Fig. 2). In addition to the cornea, the limbus, conjunctiva, and scleral rim can be evaluated as part of slit-lamp evaluation. Complete and thorough examination of the cornea can be completed in a few minutes.

One caveat of slit-lamp assessment is the relatively qualitative nature of evaluation. It is up to the technician to identify findings and then determine the severity and location to establish surgical suitability. This means the quality of evaluation can vary greatly from technician to technician if care is not taken to appropriately train the technician and maintain consistency between multiple technicians. Providing high-quality training is essential to ensuring appropriate suitability determinations. This is especially relevant because a significant portion of eye bank corneal tissue is processed; accurate baseline evaluation is needed to select appropriate tissue for processing. Using complementary technologies can facilitate more precise evaluations.

With the advent of eye banking in the 1940s through the 1980s,[3] tissue evaluation was performed almost exclusively based on the findings of thorough slit-lamp examination. This atlas shows images where slit-lamp examination alone does not yield enough information to make the most accurate suitability decisions. With the use of available and complementary technologies, eye banks can enhance slit-lamp examination and safely maximize the gift of donation.

REFERENCES

1. Eye Bank Association of America. *Medical Standards*. Washington DC: Eye Bank Association of America; 1980.
2. Eye Bank Association of America. *Medical Standards*. Washington DC: Eye Bank Association of America; 2017.
3. Aiken-O'Neill P, Mannis MJ. The evolution of eye banking in the United States: landmarks in the history of the Eye Bank Association of America. *Int J Eye Banking.* 2012;1:1–8.

Specular Microscopy

Beth Ann Benetz, CRA, FOPS, and Jonathan H. Lass, MD

(*Cornea* 2018;37:S7–S8)

The specular microscope was invented by David Maurice in the 1960s and further developed into a clinical and eye bank tool to evaluate the corneal endothelium by Bourne and Kaufman in the 1970s. The 1970s and 80s[1–3] saw research and publications exploring the normal and pathologic structure, function,[4] healing, and aging processes of the corneal endothelium[5–8] including as related to penetrating keratoplasty (PK) and the transplanted cornea.[9] Wiffen et al[10] explored the role of specular microscopy in assessment of tissue for corneal transplantation. Their conclusion was that morphologic assessment of the donor tissue probably lessens but does not eliminate the risk of primary donor failure. The 1999 Eye Bank Association of America Medical Standards state that specular microscopy "may provide useful information in screening donor tissue to determine suitability for transplantation."[11] However, it was not until 2001 that endothelial cell density (ECD) determination became adopted as a medical standard by the Eye Bank Association of America.[12] Minimal ECD requirements for suitability as a donor for corneal transplantation remain at the discretion of the local medical director. Instrument calibration on an annual basis is also a requirement of the standards.

The young, normal endothelium is observed as a single layer of finite, semipermeable hexagonal cells of similar size of the innermost layer of the cornea.[4] These cells have both a barrier and pumping action, allowing the aqueous humor to pass through and nourish the cornea while pumping out excess fluid to maintain corneal clarity.[4] With normal aging, the number of cells is slowly diminished and changes in the regularity of cell size and shape.[7] These changes are measured and reported as ECD (in cells per square millimeter), mean cell area (in square micrometers per cell), coefficient of variation (SD of cell areas/mean cell area), and percent hexagonality (percentage of 6-sided cells).[13]

After age 40 years, the normal endothelial cell layer typically has an ECD of 2500 to 3000 cells/mm^2 (Fig. 1). With most medical directors' established policy, the minimum ECD requirement for PK is 2000 cells/mm^2, whereas surgeons commonly request a higher minimum ECD (2300–2500 cells/mm^2) for endothelial keratoplasty procedures. These preferences are not necessarily based on any scientific evidence because the Specular Microscopy Ancillary Study, for example, did not show that preoperative ECD correlated with graft failure.[14] In addition, although the pattern of endothelial cell loss early on is different between PK and endothelial keratoplasty,[15] ultimately comparable cell loss is noted at 10 years in clear grafts for the 2 procedures.[16]

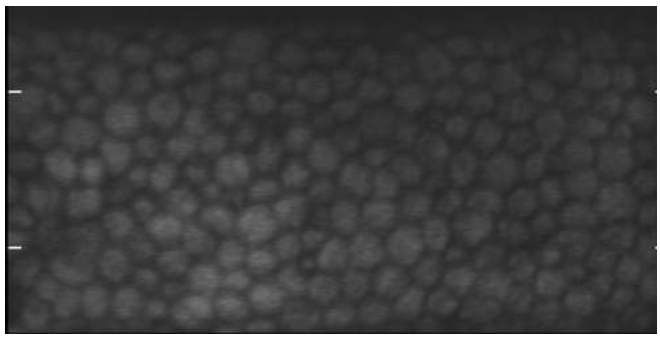

FIGURE 1. Specular microscopic image of a donor cornea endothelium with an ECD of 2637 cells/mm^2.

Trauma,[17] contact lens wear,[18] refractive surgeries,[19–21] diabetes,[22] and corneal disease[13,23–25] all impact ECD and morphology. The magnified view of the corneal endothelium with the specular microscope compared with slit-lamp examination allows qualitative assessments including evaluation of endothelial disease and possible dysfunction in the form of guttae, cell dropout, and stress. Qualitative and quantitative assessment of the endothelium are important in evaluating the suitability of the donor cornea for transplantation. The healthy donor corneal endothelium demonstrates remarkable resiliency in providing for clear corneas despite significant cell losses over time.[26]

Specular microscopes currently commercially available for eye bank use are from 2 primary manufacturers, HAI Laboratories, Inc (Lexington, MA) and Konan Medical Inc (Irvine, CA). These instruments have integrated analysis tools to determine ECD and morphologic features. Instrument calibration and understanding of analysis tools are critical for accurate determination of ECD, coefficient of variation, and hexagonality. Confounding factors in accurate analyses include tissue temperature, tissue preparation, effects of lamellar dissection, edematous cells, folds, and focus.[13] The specular images in this Atlas will demonstrate normal, pathologic, and artifact findings related to specular microscopy. Its use complementary to other technologies used in donor cornea evaluation will be demonstrated.

REFERENCES

1. Bourne WM, Kaufman HE. Specular microscopy of human corneal endothelium in vivo. *Am J Ophthalmol.* 1976;81:319–323.
2. Laing RA, Sandstrom MM, Leibowitz HM. In vivo photomicrography of the corneal endothelium. *Arch Ophthalmol.* 1975;93:143–145.

Received for publication February 28, 2018; revision received March 6, 2018; accepted March 6, 2018.

3. Maurice DM. A scanning slit optical microscope. *Invest Ophthalmol.* 1974;13:1033–1037.
4. Waring GO III, Bourne WM, Edelhauser HF, et al. The corneal endothelium: normal and pathologic structure and function. *Ophthalmology.* 1982;89:531–590.
5. Glasser DB, Matsuda M, Gager WE, et al. Corneal endothelial morphology after anterior chamber lens implantation. *Arch Ophthalmol.* 1985;103:1347–1349.
6. Laing RA. Specular microscopy of the cornea. *Curr Top Eye Res.* 1980; 3:157–218.
7. Laing RA, Sanstrom MM, Berrospi AR, et al. Changes in the corneal endothelium as a function of age. *Exp Eye Res.* 1976;22:587–594.
8. Mishima S. Clinical investigations on the corneal endothelium-XXXVIII Edward Jackson Memorial Lecture. *Am J Ophthalmol.* 1982;93:1–29.
9. Abbott RL, Fine M, Guillet E. Long-term changes in corneal endothelium following penetrating keratoplasty: a specular microscopic study. *Ophthalmology.* 1983;90:676–685.
10. Wiffen SJ, Nelson LR, Ali AF, et al. Morphologic assessment of corneal endothelium by specular microscopy in evaluation of donor corneas for transplantation. *Cornea.* 1995;14:554–561.
11. Mannis MJ, Reinhard WJ. Medical standards for eye banks. In: Brightbill FS, ed. *Corneal Surgery*. 2nd ed. St. Louis, MO: CV Mosby; 1993:531–548.
12. Eye Bank Association of America. *Medical Standards*. Washington DC: Eye Bank Association of America; 2017.
13. Sayegh RR, Benetz BA, Lass JH. Specular microscopy. In: Mannis MJ, Holland EJ, eds. *Cornea: Fundamentals, Diagnosis, Management*. New York: Elsevier; 2016:160–179.
14. Lass JH, Sugar A, Benetz BA, et al. Endothelial cell density to predict endothelial graft failure after penetrating keratoplasty. *Arch Ophthalmol.* 2010;128:63–69.
15. Price MO, Gorovoy M, Benetz BA, et al. Descemet's stripping automated endothelial keratoplasty outcomes compared with penetrating keratoplasty from the Cornea Donor Study. *Ophthalmology.* 2010;117: 438–444.
16. Price MO, Calhoun P, Kollman C, et al. Descemet stripping endothelial keratoplasty: ten-year endothelial cell loss compared with penetrating keratoplasty. *Ophthalmology.* 2016;123:1421–1427.
17. Roberson MC, Wicheta WE. Endothelial loss in corneal concussion injury. *Ann Ophthalmol.* 1985;17:457–458, 460.
18. Tseng SH, Yu CH, Wang ST. [Morphometric analysis of corneal epithelium in normal subjects and soft contact lens wearers]. *J Formos Med Assoc.* 1995;94(suppl 1):S20–S25.
19. Collins MJ, Carr JD, Stulting RD, et al. Effects of laser in situ keratomileusis (LASIK) on the corneal endothelium 3 years postoperatively. *Am J Ophthalmol.* 2001;131:1–6.
20. Mardelli PG, Piebenga LW, Matta CS, et al. Corneal endothelial status 12 to 55 months after excimer laser photorefractive keratectomy. *Ophthalmology.* 1995;102:544–549; discussion 548–549.
21. Spadea L, Dragani T, Blasi MA, et al. Specular microscopy of the corneal endothelium after excimer laser photorefractive keratectomy. *J Cataract Refract Surg.* 1996;22:188–193.
22. Pardos GJ, Krachmer JH. Comparison of endothelial cell density in diabetics and a control population. *Am J Ophthalmol.* 1980;90:172–174.
23. Hirst LW, Waring GO III. Clinical specular microscopy of posterior polymorphous endothelial dystrophy. *Am J Ophthalmol.* 1983;95: 143–155.
24. Takahashi N, Sasaki K, Nakaizumi H, et al. Specular microscopic findings of lattice corneal dystrophy. *Int Ophthalmol.* 1987;10:47–53.
25. Waring GO III, Rodrigues MM, Laibson PR. Corneal dystrophies. II. Endothelial dystrophies. *Surv Ophthalmol.* 1978;23:147–168.
26. Lass JH, Benetz BA, Gal RL, et al. Donor age and factors related to endothelial cell loss 10 years after penetrating keratoplasty: Specular Microscopy Ancillary Study. *Ophthalmology.* 2013;120: 2428–2435.

Anterior Segment Optical Coherence Tomography

Adam Stockman, CEBT

(*Cornea* 2018;37:S9–S10)

Historically, obtaining accurate measurement of corneal pachymetry was not a critical part of tissue evaluations performed by the eye bank. Simply noting the presence and perceived severity of stromal edema with increased corneal thickness would be reported as part of slit-lamp evaluation of a cornea. However, as endothelial keratoplasty began to become more common around 2006, accurate corneal pachymetry of donor tissue became increasingly important (Fig. 1).[1]

In the mid-2000s, when donor preparation for Descemet stripping automated endothelial keratoplasty (DSAEK) began being performed in the eye bank setting, the ability to accurately measure corneal thickness became critical.[2–4] Early adopters relied on handheld pachymeter units to obtain accurate readings of corneal thickness at the time of tissue processing. Although these handheld units provided eye banks with accurate pachymetry, they were not without issue.

Because pachymetry was performed at the same time as DSAEK preparation, an eye bank may not know that a cornea is too thick or too thin to process until the cornea had already been removed from its storage solution and mounted on an artificial anterior chamber. The use of the handheld unit during processing also extended the time a cornea spent out of storage solution and required the processing eye bank to touch a nonsterile probe to the cornea to obtain readings.

The ability to obtain accurate thickness measurement before DSAEK processing became increasingly important as surgeon preferences for final DSAEK graft thicknesses became more specific.[5] Specular microscopes have the ability to measure corneal thickness through obtaining an in-focus image of the endothelium and an in-focus image of the epithelium and measuring the distance the stage travels between those images. This provided the advantage of knowing the corneal thickness before processing; however, because of the subjectivity of technicians, it was difficult to measure only epithelial thickness and often times still required the use of a handheld pachymeter unit during processing.

With the increasing need to know corneal thickness with a high degree of accuracy (including being able to precisely measure the thickness of the corneal epithelium),

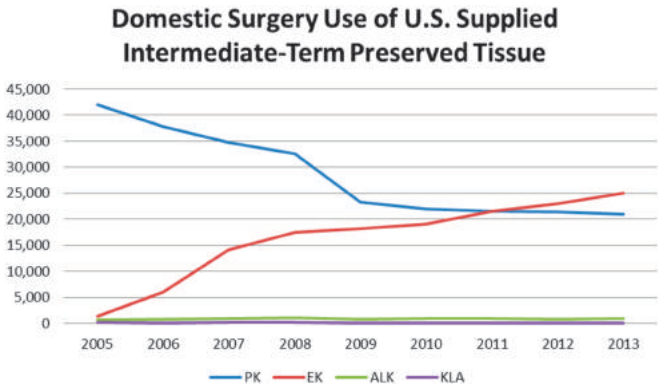

FIGURE 1. Increasing demand for EK expands demand for OCT. Image courtesy of the Eye Bank Association of America. ALK, anterior lamellar keratoplasty; EK, endothelial keratoplasty; KLA, keratolimbal allograft; PK, penetrating keratoplasty.[1]

eye banks began using optical coherence tomography (OCT) in the late 2000s.[6] The first adopters of this technology immediately saw tremendous benefit in obtaining OCT images before processing tissue and further benefit in integrating the use of OCT in routine evaluation of donor tissue (Fig. 2).

The most widely adopted OCT model used by contributors of images for this Atlas was the Optovue RTVue (Fremont, CA) (Fig. 3). Other OCT models included the Envisu R Series SDOCT (Leica Microsystems Inc, Buffalo Grove, IL) and the Carl Zeiss Visante (Dublin, CA). All of these models give eye bank personnel the ability to accurately analyze donor corneas to determine their suitability for various surgical uses.

Beyond accurate measurement of corneal thickness (Fig. 4), OCT imagery allows for highly accurate

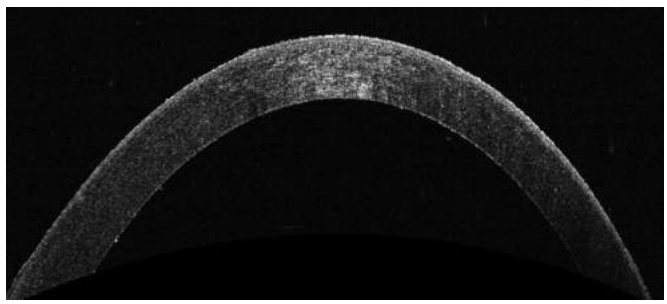

FIGURE 2. OCT image of a cornea before tissue processing.

Received for publication February 28, 2018; revision received March 6, 2018; accepted March 6, 2018.

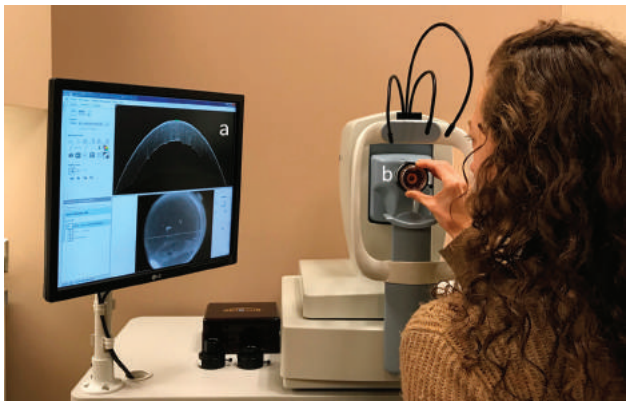

FIGURE 3. RTVue OCT (Optovue, Fremont, CA) as set up in an eye bank. A, Customized software is designed for analyzing corneal tissue in preservation medium. B, An adaptor for cornea viewing chambers makes tissue positioning easy. The operator makes fine adjustments and then can lock the chamber in place with an adjustment screw.

measurements of anterior scars to determine whether a cornea can be processed for use in DSAEK preparation.[7] OCT imagery also allows eye bank personnel to accurately measure the stroma and epithelium separately. Armed with this knowledge, eye bank personnel can develop a detailed plan before processing such as determining the appropriate microkeratome head size or whether to remove the epithelium before processing. With a plan in place, eye banks are able to provide DSAEK grafts within the requested thickness parameters. OCT can also be used to identify potential stromal infiltrates, distinguished from simple epithelial exposure. And finally, OCT may aid eye banks in screening for refractive surgery.[8]

OCT imagery has become an important addition to the eye banking community's tool kit to continue to ensure that appropriate donor corneas are being provided for surgical use. This atlas will illustrate its usage in various eye banking situations and how it complements other donor cornea evaluation technologies.

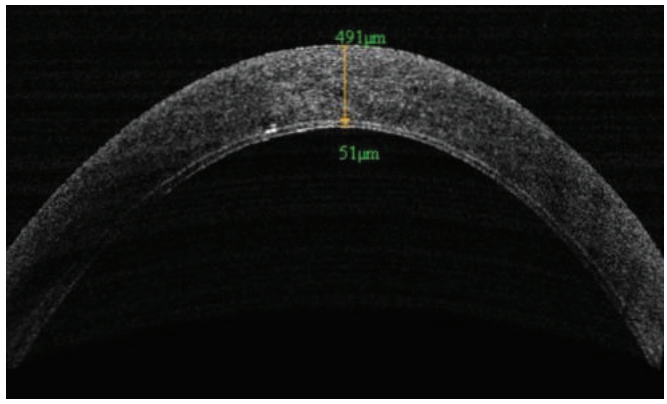

FIGURE 4. OCT cross section of a donor cornea prepared for Descemet membrane automated endothelial keratoplasty (DSAEK). Graft thickness is measured at 51 μm, and the graft profile is observed.

REFERENCES

1. Eye Bank Association of America. *2013 Eye Banking Statistical Report*. 2014. http://restoresight.org/wp-content/uploads/2016/03/2015-Statistical-Report.pdf. Accessed November 2, 2017.
2. Brown JS, Wang D, Li X, et al. In situ ultrahigh-resolution optical coherence tomography characterization of eye bank corneal tissue processed for lamellar keratoplasty. *Cornea.* 2008;27:802–810.
3. Tang M, Stoeger C, Galloway J, et al. Evaluating DSAEK graft deturgescence in preservation medium after microkeratome cut with optical coherence tomography. *Cornea.* 2013;32:847–850.
4. Woodward MA, Titus MS, Shtein RM. Effect of microkeratome pass on tissue processing for Descemet stripping automated endothelial keratoplasty. *Cornea.* 2014;33:507–509.
5. Neff KD, Biber JM, Holland EJ. Comparison of central corneal graft thickness to visual acuity outcomes in endothelial keratoplasty. *Cornea.* 2011;30:388–391.
6. Eye Bank Association of America. *Medical Standards*. Washington, DC: Eye Bank Association of America; 2017.
7. Bald MR, Stoeger C, Galloway J, et al. Use of Fourier-domain optical coherence tomography to evaluate anterior stromal opacities in donor corneas. *J Ophthalmol.* 2013;2013:397680.
8. Lin RC, Li Y, Tang M, et al. Screening for previous refractive surgery in eye bank corneas by using optical coherence tomography. *Cornea.* 2007; 26:594–599.

Wide-Field Ex Vivo Dual Imaging Microscopy

Kayla E. Gray, CCRP

(*Cornea* 2018;37:S11–S13)

Since the introduction of specular microscopy clinically into eye banks in the 1970s,[1–3] this imaging technology has been primarily limited to imaging of the central corneal endothelium for determination of endothelial cell density (ECD), morphology (coefficient of variation and % of hexagonal cells), and detection of disease at a more magnified view than afforded by slit-lamp examination. Confocal microscopy,[4] available clinically for patients, accomplishing not only endothelial imaging but cross-sectional imaging across the entire cornea, was never commercially available in eye banking.

This limitation has now changed with the introduction in 2015 of a "confocal image–like" wide-field ex vivo dual imaging microscope (CellChek® D+®; Konan Medical, Irvine, CA).[5] This image atlas is the first major effort to demonstrate the capabilities of this instrument and the potential for its uses complementing slit-lamp biomicroscopy, conventional specular microscopy, and optical coherence tomography imaging. To our knowledge, this new technology is the first multi-imaging system for donor corneas. As defined by the manufacturer, it uses a specular microscopy mode (Specular mode), an Enhanced mode, and a Finder mode to better image and evaluate the cornea ex vivo.[5] According to the manufacturer, the Specular mode has an expanded viewing area of 750,000 μm^2.[5] With the larger viewing field, the microscope allows users to visualize all the corneal layers in a cross-sectional view across the entire cornea.[6] For endothelial imaging and determination of ECD, an option to sample and analyze 4 different areas of the central and midperipheral endothelium is possible. The average ECD can then be determined with a potential area of analysis of 480,000 μm^2, allowing for an 8.5× larger analysis field compared to its predecessor, the Konan EB-10.[6] The dual imaging microscope also allows for a 10-degree greater tilt to better account for the curvature of the cornea when analyzing samples (Figs. 1–4).[5]

Beyond the advancements associated with specular microscopy, the Enhanced mode provides confocal image–like or "scanning electron microscopy–like" imaging of all corneal layers such as imaging from the irregular surface of the epithelium, endothelium, and interface of lamellar dissection of the donor for Descemet stripping automated endothelial keratoplasty with a 3-dimensional effect, a limitation of conventional specular microscopy.[5] With its introduction in 2015, these capabilities are now being explored by eye banks and corneal surgeons as to its utility with both normal and disease states affecting these layers. Because the

FIGURE 1. Wide-field ex vivo dual imaging microscope. Reprinted from Konan Medical.[5]

Received for publication February 28, 2018; revision received March 6, 2018; accepted March 6, 2018.

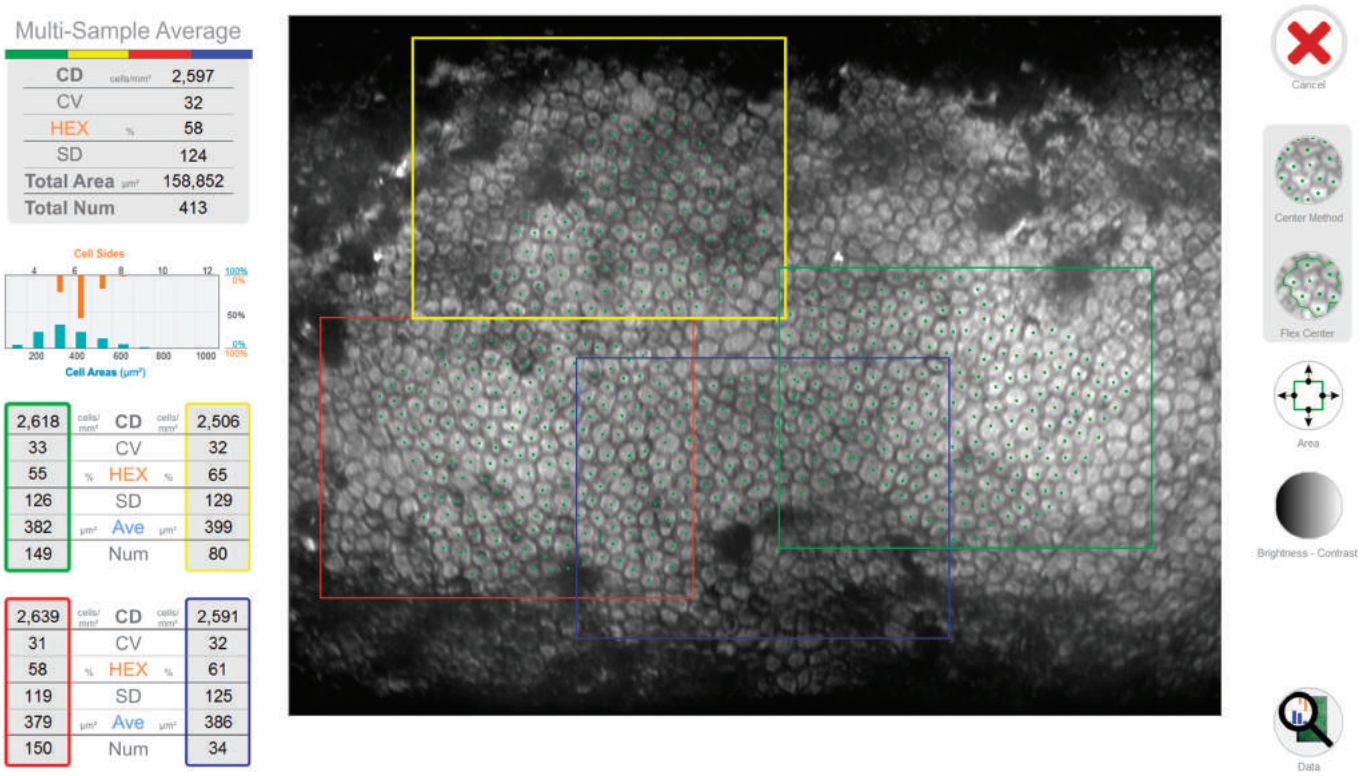

FIGURE 2. Wide-field ex vivo dual imaging Specular mode. Reprinted from Konan Medical.[5]

Enhanced mode enables seeing the surface of the outer epithelium, the apical surface of the endothelium and the interface of lamellar dissection, total corneal thickness, or graft thickness can also be measured. Once the Enhanced mode image is captured, a composite image can display the Enhanced mode and Specular mode images over each other to better define the cornea's pathology.

The Finder mode (low magnification) allows users to see the overall appearance of the entire donor cornea with reference location indication. This new view provides the ability to scan the donor cornea and determine the areas of interest for further analysis by switching to the high-magnification view. This mode also allows users to determine the diameter of the cornea or clear zone and the lengths and areas of any area of interest on the cornea using donor feature measurement tools.[5]

The newly introduced wide-field ex vivo dual imaging microscope has provided an imaging tool whose contribution to the tissue evaluation process remains to be fully explored and has not yet become part of the standard operating procedure of the eye bank. It is the hope of the coeditors and contributors of this atlas that the images from this instrument, as they complement the images from other existing technologies, will stimulate establishment of

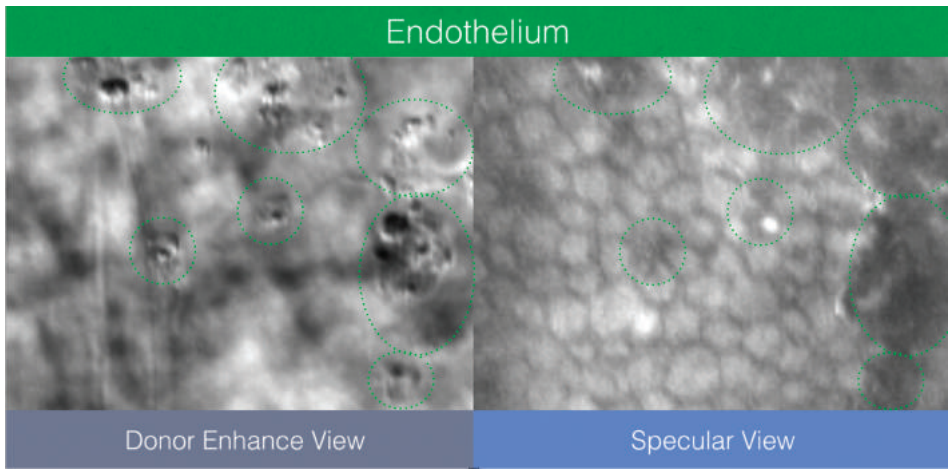

FIGURE 3. Wide-field ex vivo dual imaging comparison of Enhanced and Specular modes. Reprinted from Konan Medical.[5]

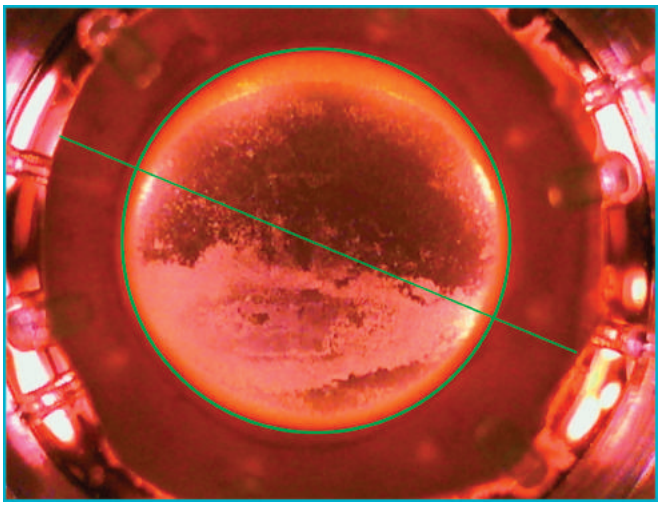

FIGURE 4. Wide-field ex vivo dual imaging Finder mode with measurement tools. Reprinted from Konan Medical.[5]

specific guidelines and procedures for incorporation of this new imaging technology into standard operating procedure to further enhance tissue evaluation for the 21st century eye bank, assuring the highest tissue quality and inclusion of more tissues which may have been eliminated based on slit-lamp examination alone.

REFERENCES

1. Bourne WM, Kaufman HE. Specular microscopy of human corneal endothelium in vivo. *Am J Ophthalmol.* 1976;81:319–323.
2. Laing RA, Sandstrom MM, Leibowitz HM. In vivo photomicrography of the corneal endothelium. *Arch Ophthalmol.* 1975;93:143–145.
3. Maurice DM. A scanning slit optical microscope. *Invest Ophthalmol.* 1974;13:1033–1037.
4. Guthoff RF, Zhivov A, Stachs O. In vivo confocal microscopy, an inner vision of the cornea: a major review. *Clin Exp Ophthalmol.* 2009;37:100–117.
5. Konan Medical. CellChek D donor corneal analysis. Available at: https://konanmedical.com/cellchek-d/. Accessed November 17, 2017.
6. Tran KD, Clover J, Odell K, et al. Comparison of endothelial cell measurements by two eye bank specular microscopes. *Int J Eye Banking.* 2016;4:1–8.

Comparative Image Atlas of Current and New Technologies in Corneal Donor Tissue Evaluation

This image atlas is organized to display images of the normal donor cornea and all its layers, the diseased cornea by layers affected, the appearance of the corneal layers after donor preparation for Descemet stripping endothelial keratoplasty and Descemet membrane endothelial keratoplasty, the effect of tissue warming, and finally other interesting findings. Each image set is organized in the order by how the eye bank technician with access to all these technologies might approach tissue evaluation as applicable for the tissue condition being evaluated: slit-lamp examination, conventional specular microscopy, optical coherence tomography, and the newest technology, wide-field ex vivo dual imaging microscopy. In some cases, image sets do not demonstrate all available modalities. Care was taken to show those modalities that are most illustrative of a given condition.

List of Figures

Received for publication February 28, 2018; revision received March 6, 2018; accepted March 6, 2018.

Normal Cornea

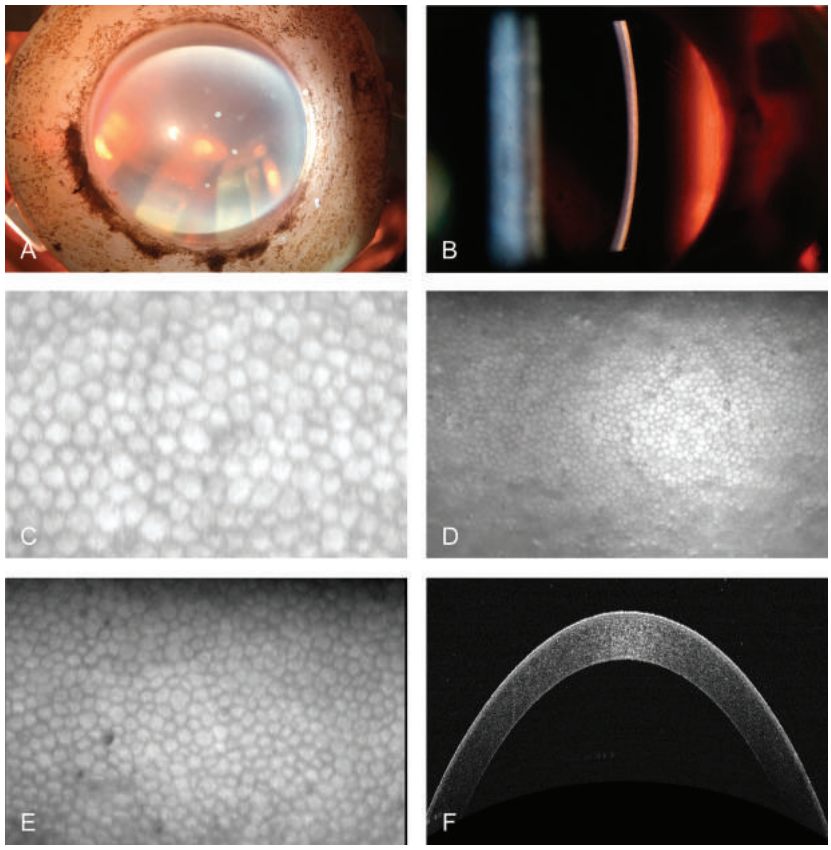

FIGURE 1. Normal cornea. A, Diffuse Topcon SL-4ED slit-lamp view, low magnification. B, The Fine Topcon SL-4ED slit beam shows compact stroma. C, Konan EB-10 specular microscopic image demonstrates a view of cells demonstrating the regular size and shape. D, Konan wide-field ex vivo dual imaging specular microscopy demonstrates a view of cells demonstrating the regular size and shape. E, HAI EB-2000xyz specular microscopic image demonstrates a view of cells demonstrating the regular size and shape. F, Optovue RTVue 100 optical coherence tomography distinctly demonstrates the compact stroma, hyperreflective epithelium, Bowman membrane, and endothelium.

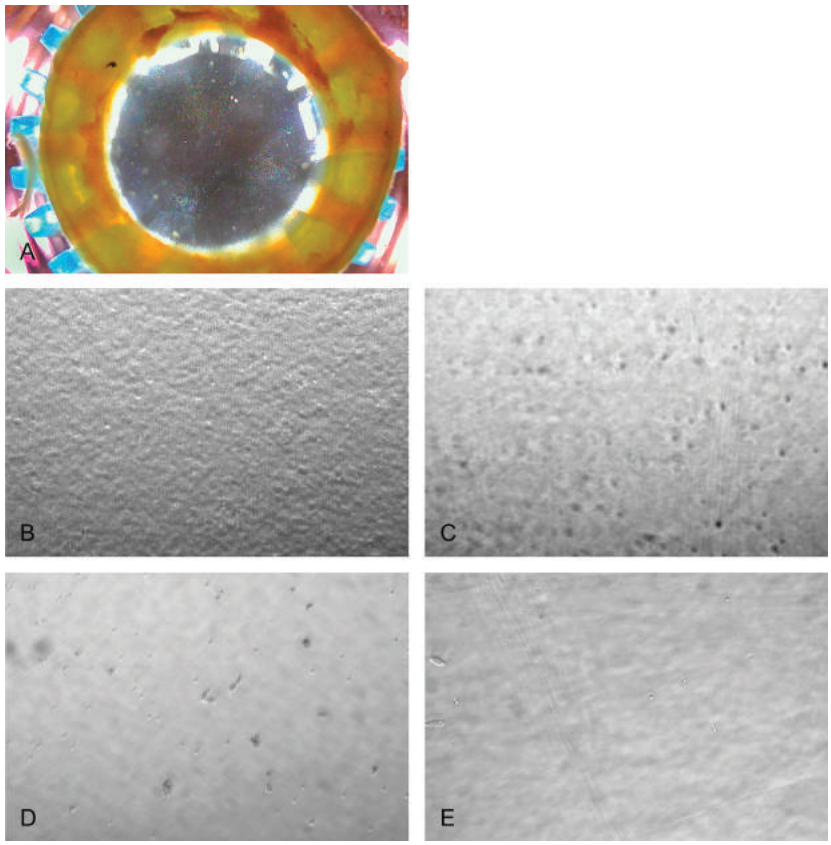

FIGURE 2. Normal cornea. A, The Finder mode of the Konan wide-field ex vivo dual imaging specular microscopy shows a clear cornea with minimal epithelial exposure. B, The Enhanced mode of the Konan wide-field ex vivo dual imaging specular microscopy shows a normal epithelium. C, The Enhanced mode of the Konan wide-field ex vivo dual imaging specular microscopy shows normal stroma. D, The Enhanced mode of the Konan wide-field ex vivo dual imaging specular microscopy shows normal Descemet membrane. E, The Enhanced mode of the Konan wide-field ex vivo dual imaging specular microscopy shows a normal endothelial layer.

Epithelium

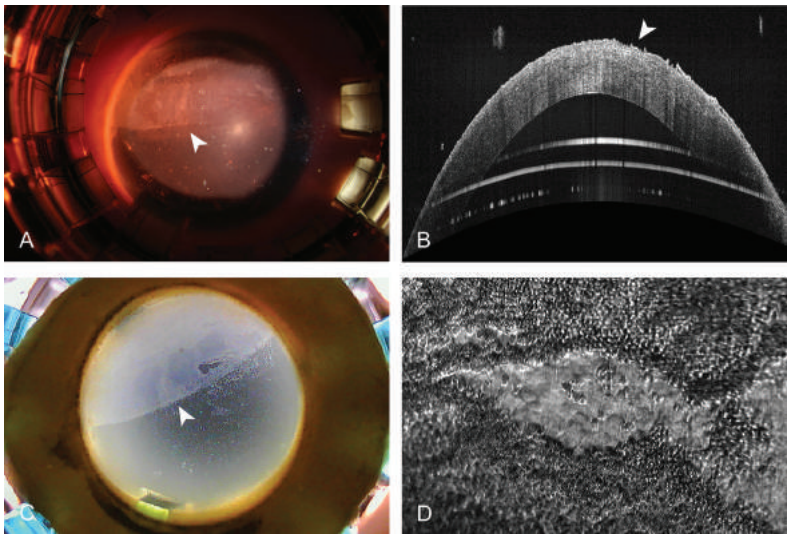

FIGURE 3. Epithelial exposure. A, Diffusely illuminated slit-lamp view. The arrow points to lid line exposure. B, Optical coherence tomography showing a disrupted epithelium. The arrow points to the area of sloughed epithelial cells. C, The Finder mode provides clear demarcation noted by the arrow of an intact versus nonintact epithelium. D, The Enhanced mode shows the denuded area of the epithelium adjacent to the areas of epithelial cells.

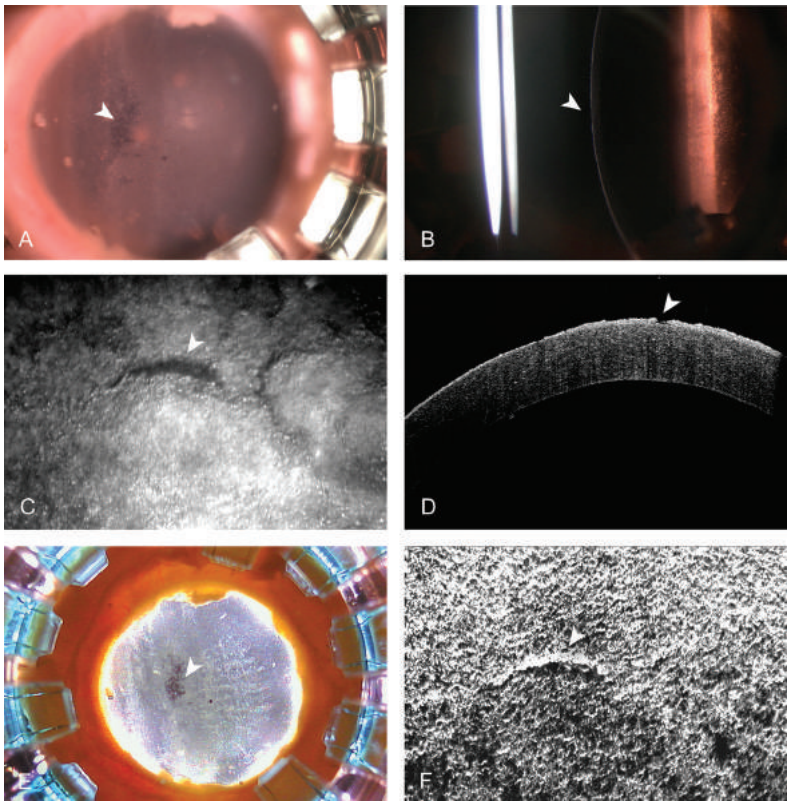

FIGURE 4. Epithelial defect. A and B, A wide slit beam provides indirect illumination highlighting the epithelial defect (arrows). C, The Konan wide-field ex vivo dual imaging specular microscopic image of the epithelium highlights the epithelial defect (arrow). D, Optical coherence tomography shows the thickened and irregular epithelium with the epithelial defect (arrow). E, The Finder mode shows distribution of the epithelial defect (arrow). F, The Enhanced mode demonstrates epithelial cell damage and edema consistent with the defect noted previously (arrow).

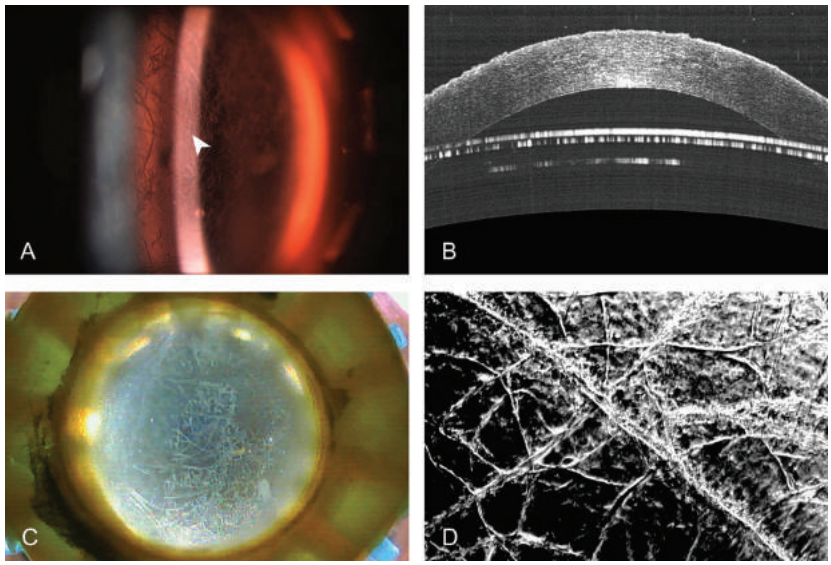

FIGURE 5. Heavy superficial punctate keratitis. A, A slit-lamp view shows heavy linear punctate epithelial defects. The arrow points to the area of interest. B, Optical coherence tomography shows a highly irregular epithelium. C, The Finder mode also shows an area across the cornea with heavy linear punctate epithelial defects. D, The Enhanced mode shows the heavy linear punctate epithelial defects.

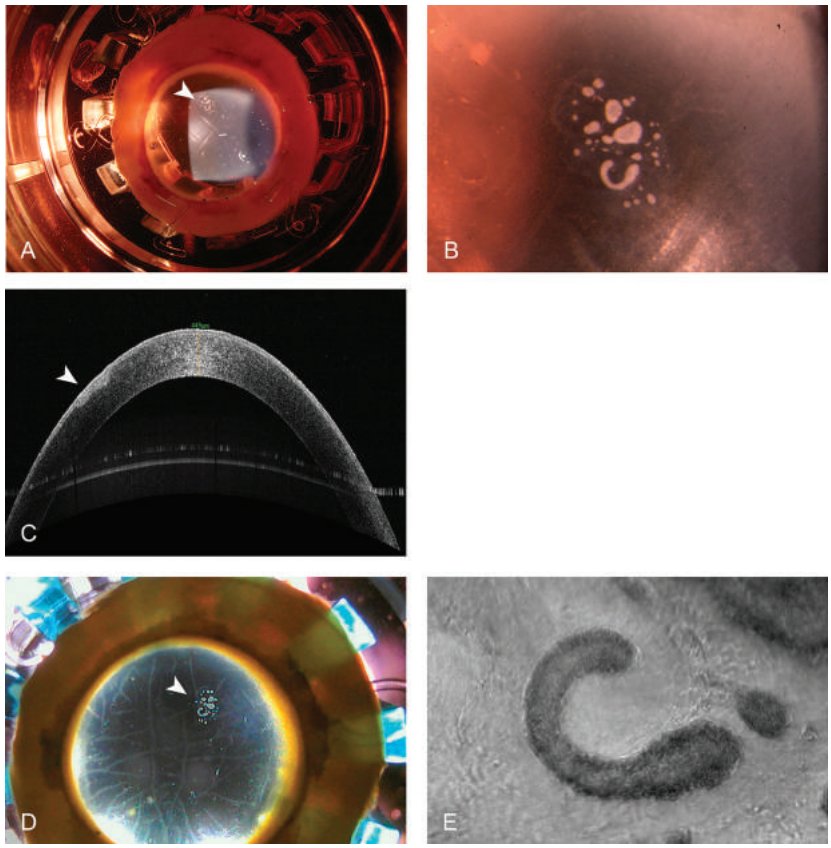

FIGURE 6. Map dot fingerprint dystrophy (MDF). A, Diffuse, low-magnification slit-lamp image of MDF dystrophy epithelial abnormalities. The arrow points to the area of interest. B, High-magnification slit-lamp image of epithelial abnormality. C, Optical coherence tomography shows MDF dystrophic changes (arrow). D, The Finder mode highlights epithelial abnormality (arrow). E, The Enhanced mode shows a normal epithelium with adjacent MDF abnormality (dark area).

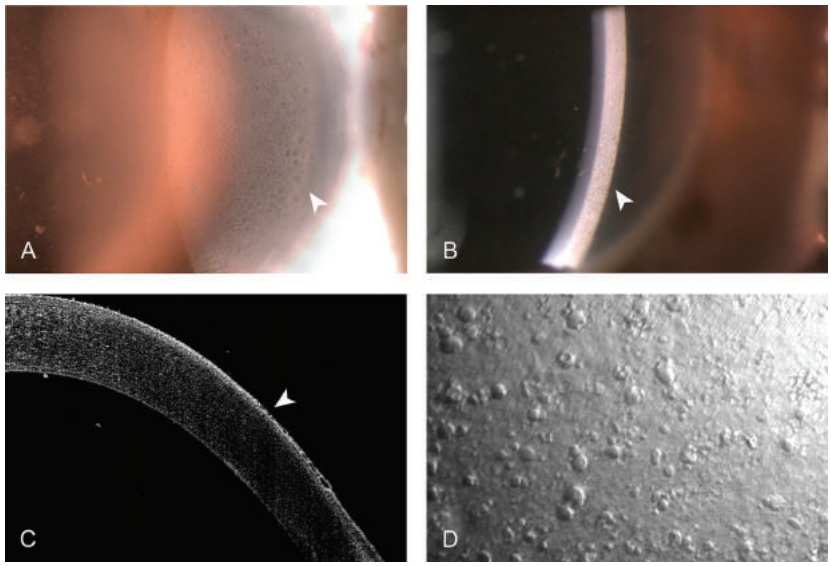

FIGURE 7. Meesmann dystrophy. A, Diffuse slit-lamp image with an arrow pointing toward the area of diffuse cystic changes in the epithelium. B, Narrow slit beam with an arrow highlighting diffuse cystic changes in the epithelium. C, Optical coherence tomography showing a cross section of the epithelium demonstrating epithelial irregularity related to the cystic epithelial changes (arrow). D, Enhanced mode of the epithelium showing the raised nature of cysts.

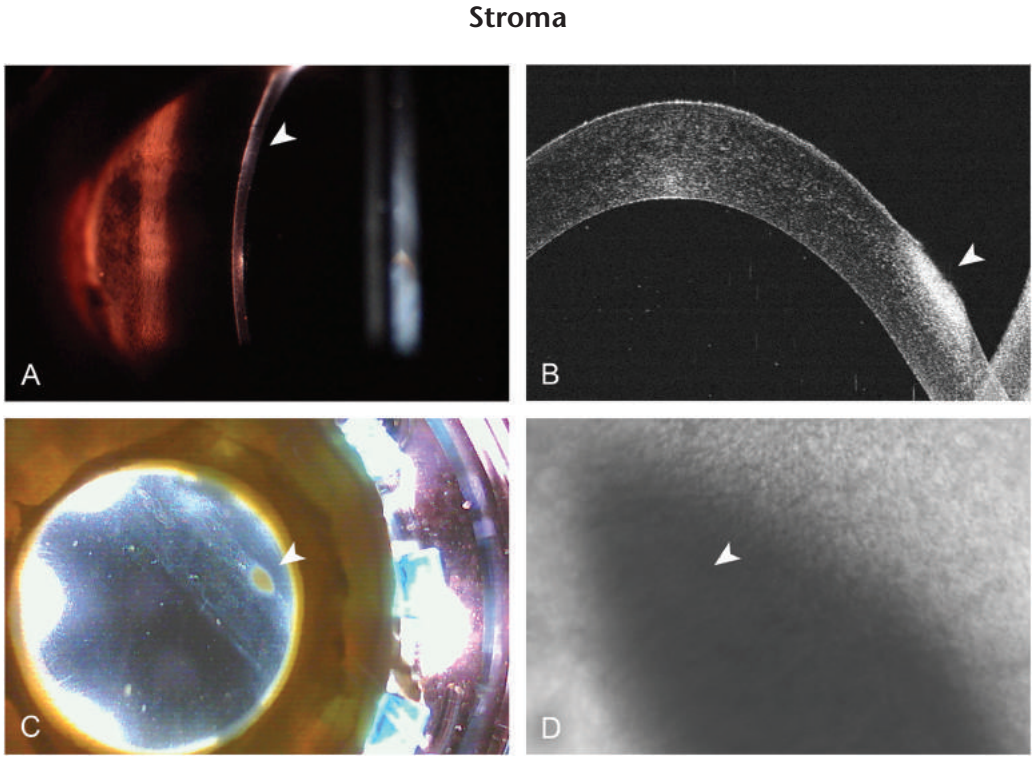

FIGURE 8. Stromal infiltrate. A, Fine slit beam demonstrating focal infiltrate extending into stroma. The arrow points to the area of interest. B, Optical coherence tomography showing a break in the epithelium and hyper-reflectivity in stroma consistent with an infiltrate (arrow). C, The Finder mode shows the focal infiltrate location in the peripheral cornea along a band of epithelial exposure (arrow). D, The Enhanced mode of stroma shows the opaque nature of the infiltrate differentiating it from the normal adjacent stroma (arrow).

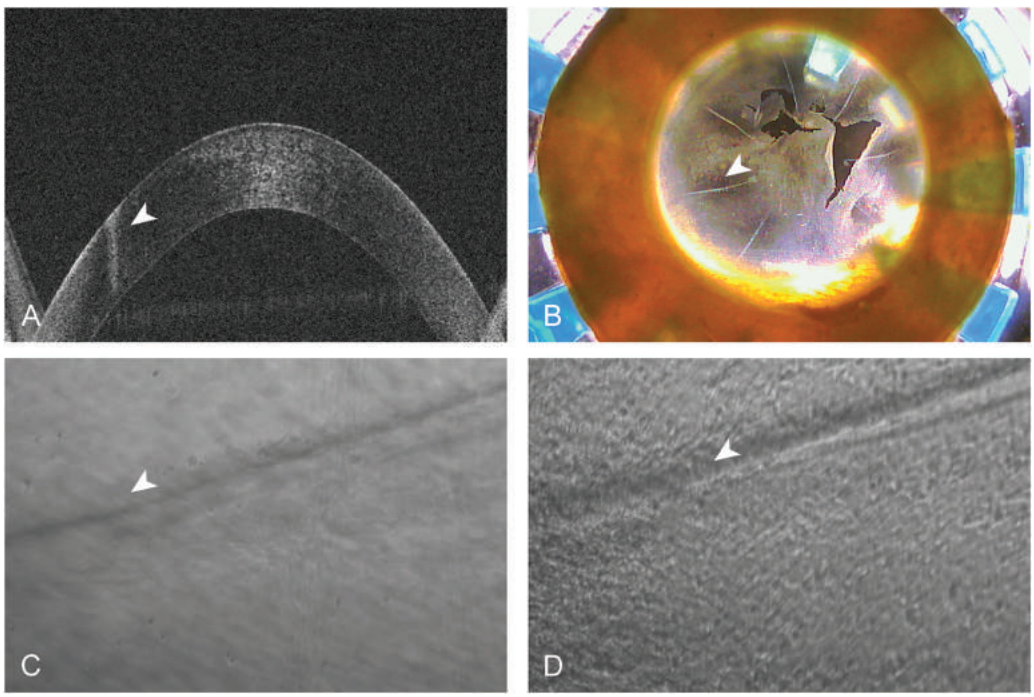

FIGURE 9. Radial keratotomy scars. A, Optical coherence tomography showing a nearly full-depth stromal scar (arrow). B, The Finder mode shows distribution of scars (the arrow points to a representative scar) and severe epithelial sloughing. C, The Enhanced mode of the endothelium shows the depth of radial keratotomy scars (arrow). D, The Enhanced mode of the epithelium shows the depth of radial keratotomy scars (arrow).

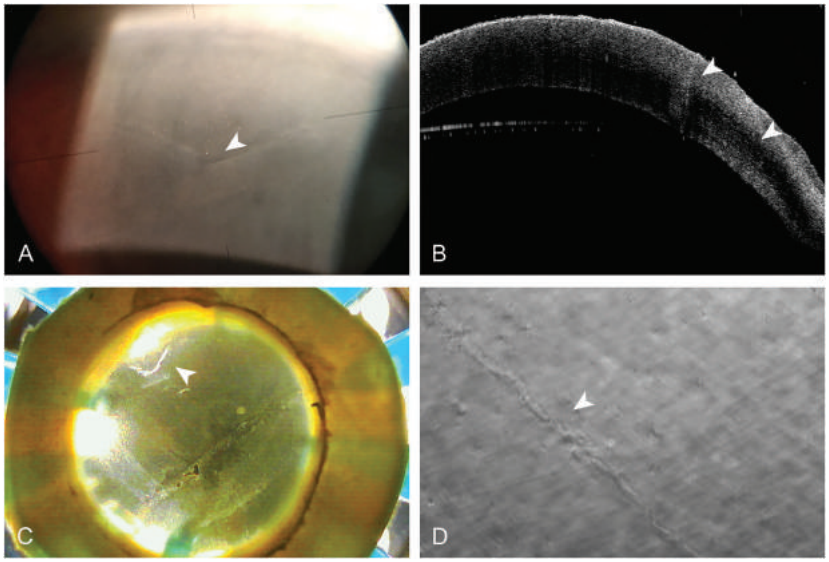

FIGURE 10. IOL surgical scars. A, Wide slit beam with disruption in Descemet membrane and reflective particles (arrow). B, Optical coherence tomography showing full thickness stromal scarring from surgical incisions (arrows). C, The Finder mode clearly shows the location of the surgical wound (arrow). D, The Enhanced mode shows disruption in Descemet membrane at the site of the surgical scar (arrow).

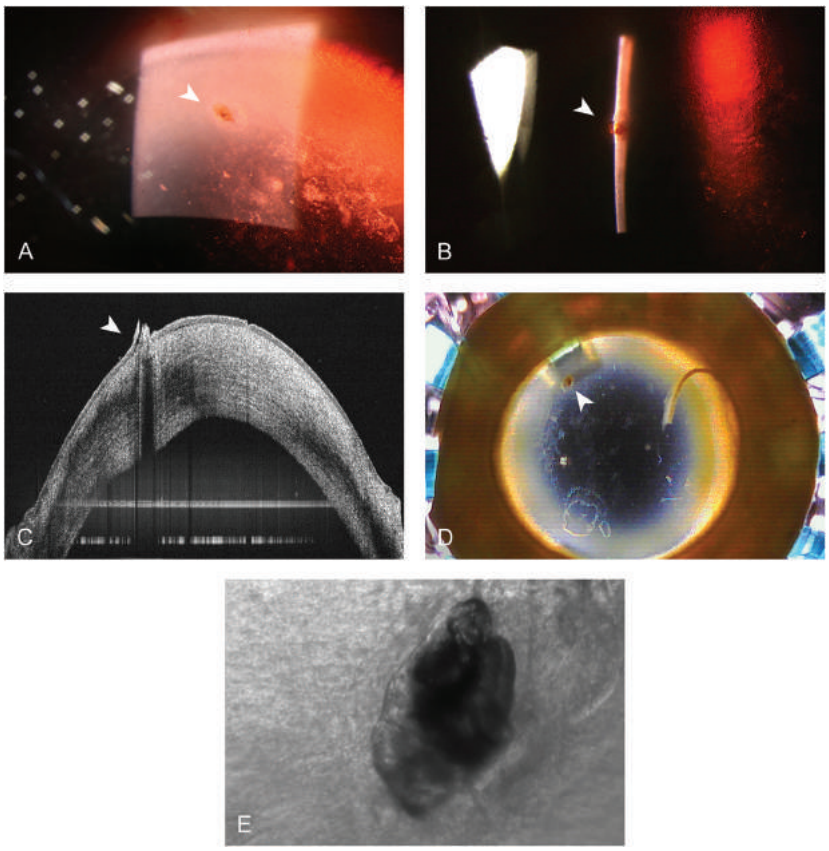

FIGURE 11. Stromal foreign body. A and B, Wide and narrow slit beams highlight a foreign body (arrows). C, Optical coherence tomography shows the depth of the foreign body (arrow). D, The Finder mode shows the location of the foreign body (arrow). E, The Enhanced mode shows a high-magnification view of the foreign body.

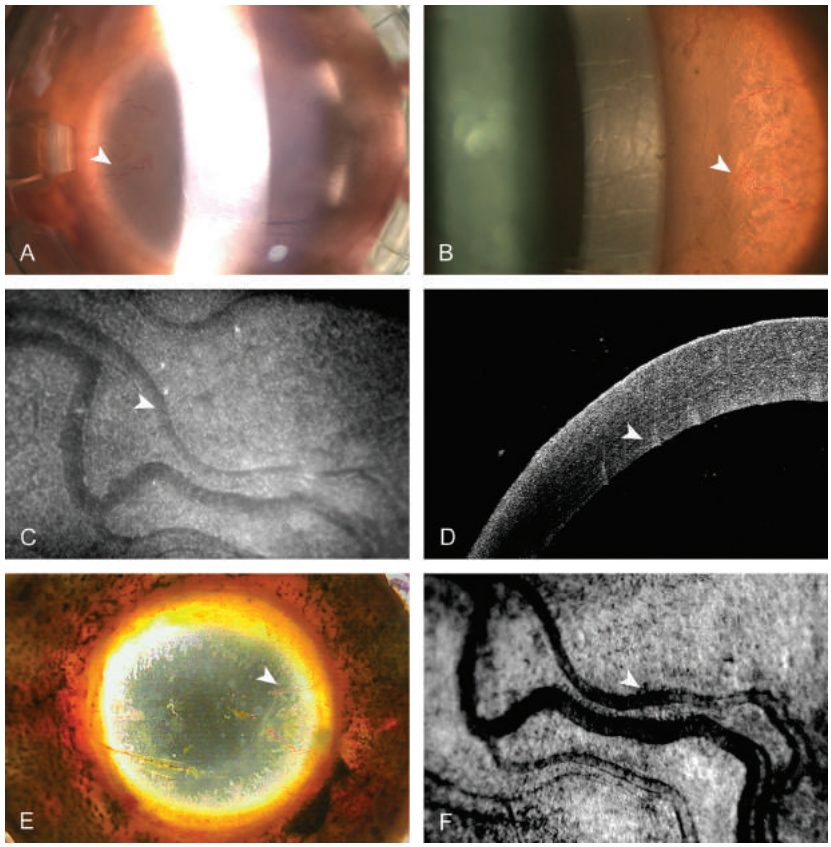

FIGURE 12. Stromal vascularization. A and B, Indirect slit-lamp illumination highlights deep peripheral stromal vascularization (arrows). C, Konan wide-field ex vivo dual imaging Specular mode of stromal vessels (arrow). D, Optical coherence tomography with the faint view of vessels (arrow). E, The Finder mode shows peripheral stromal vascularization (arrow). F, The Enhanced mode shows stromal vessels (arrow).

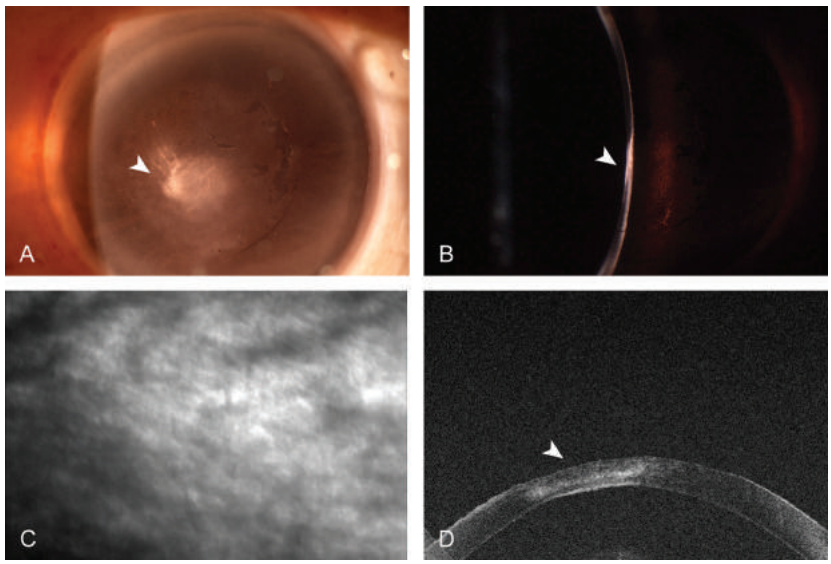

FIGURE 13. Fungal elements with stromal keratitis. A and B, Diffuse and wide slit beams demonstrate central stromal infiltrate (arrows). C, HAI Specular mode of fungal elements shows the specular reflected light resulting in a scatter, due to the nature of the fungal infection. D, Optical coherence tomography shows midstromal infiltrate (arrow).

Descemet's Membrane

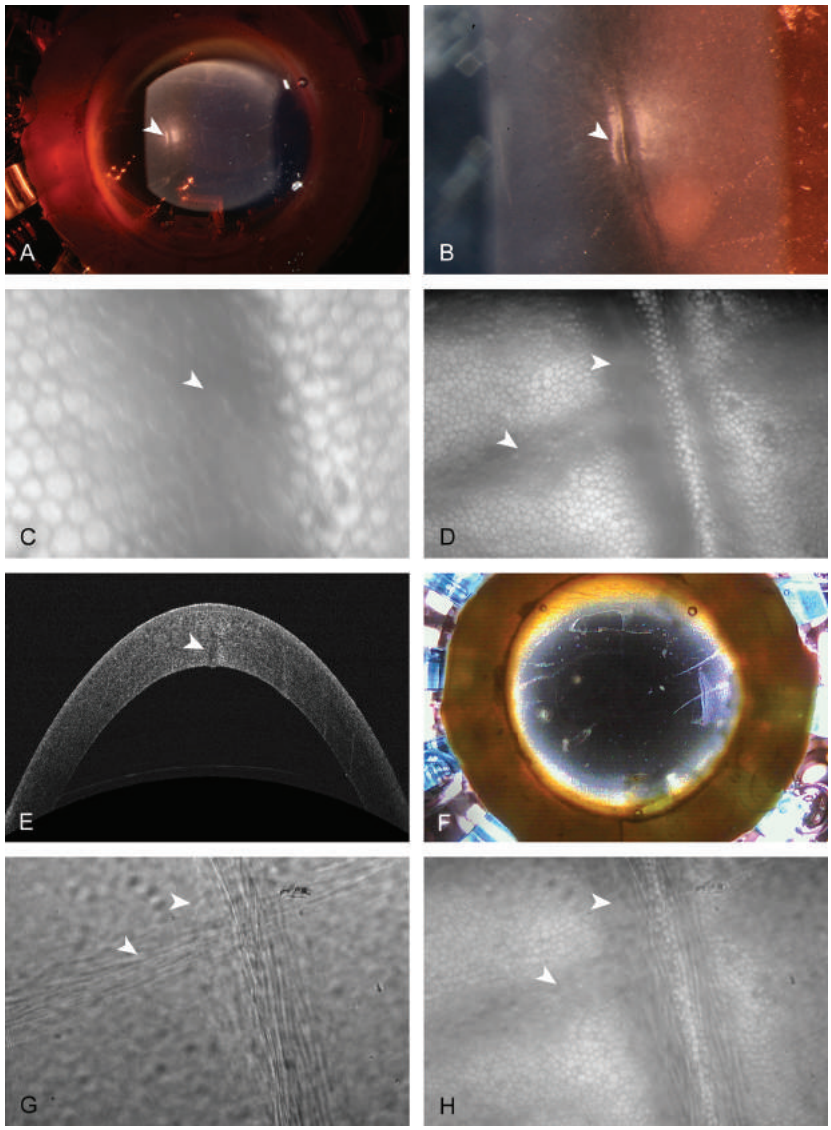

FIGURE 14. Descemet folds. A and B, A wide slit-lamp beam at low and high magnifications shows localized Descemet folds (arrows). C, Konan EB-10 specular microscopy image of Descemet folds (arrow). D, Konan wide-field ex vivo dual imaging specular microscopy image of Descemet folds (arrows). E, Optical coherence tomography shows stromal edema with associated Descemet folds (arrow). F, The Finder mode does not contribute to visualization of folds. G, The Enhanced mode shows disruption in the endothelial layer at the fold (arrows). H, Combining enhanced and Konan wide-field ex vivo dual imaging specular microscopy in a composite image demonstrates folding in Descemet membrane (arrows). Dark areas are zones of Descemet membrane out of the plane of specular reflection due to folding.

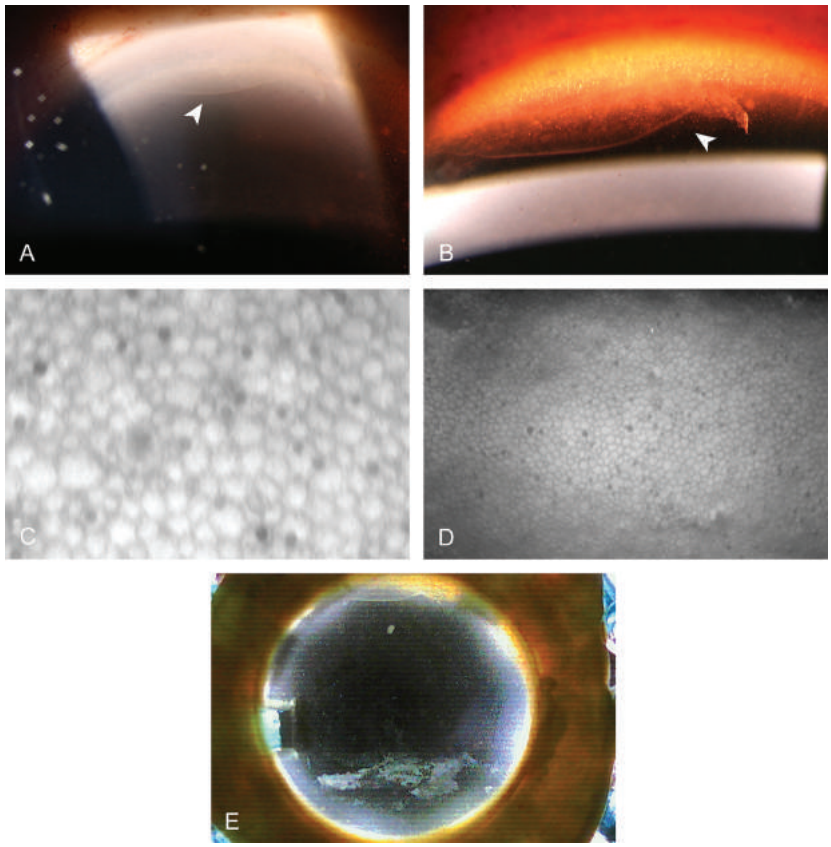

FIGURE 15. Descemet detachment. A and B, Peripheral Descemet detachment is seen with a wide slit (arrows). C, Konan EB-10 specular microscopy demonstrates intact endothelial cells centrally despite detached peripheral Descemet membrane. D, Konan wide-field ex vivo dual imaging specular image microscopy demonstrates intact endothelial cells centrally despite detached peripheral Descemet membrane. E, The Finder mode allows for easy location of the peripheral Descemet detachment.

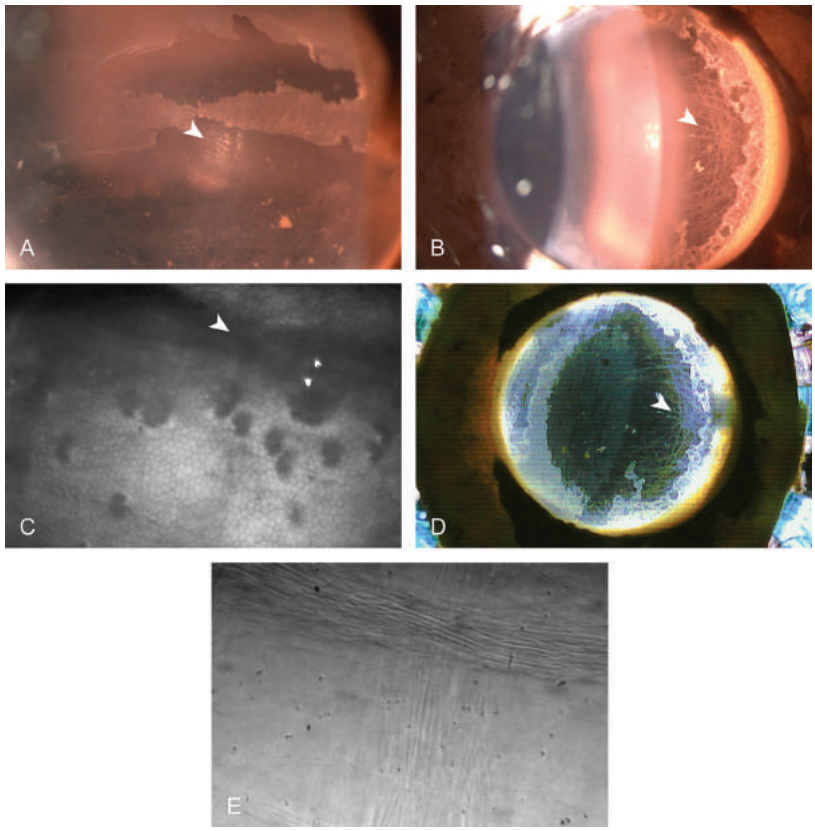

FIGURE 16. Corneal edema with folds (defect). A, Diffuse slit-lamp illumination reveals endothelial folds seen with specular reflection (arrow). There is also a large epithelial defect. B, Indirect illumination demonstrates diffuse peripheral endothelial edema and folds (arrow). C, Konan wide-field ex vivo dual imaging specular microscopy shows endothelial damage in a linear pattern of a dark, nonreflective area (arrow) surrounded by visibly intact cells. D, The Finder mode shows endothelial stress lines (arrow). E, The Enhanced mode shows the collagen fibers associated with greater corneal edema and surrounding cell dropout.

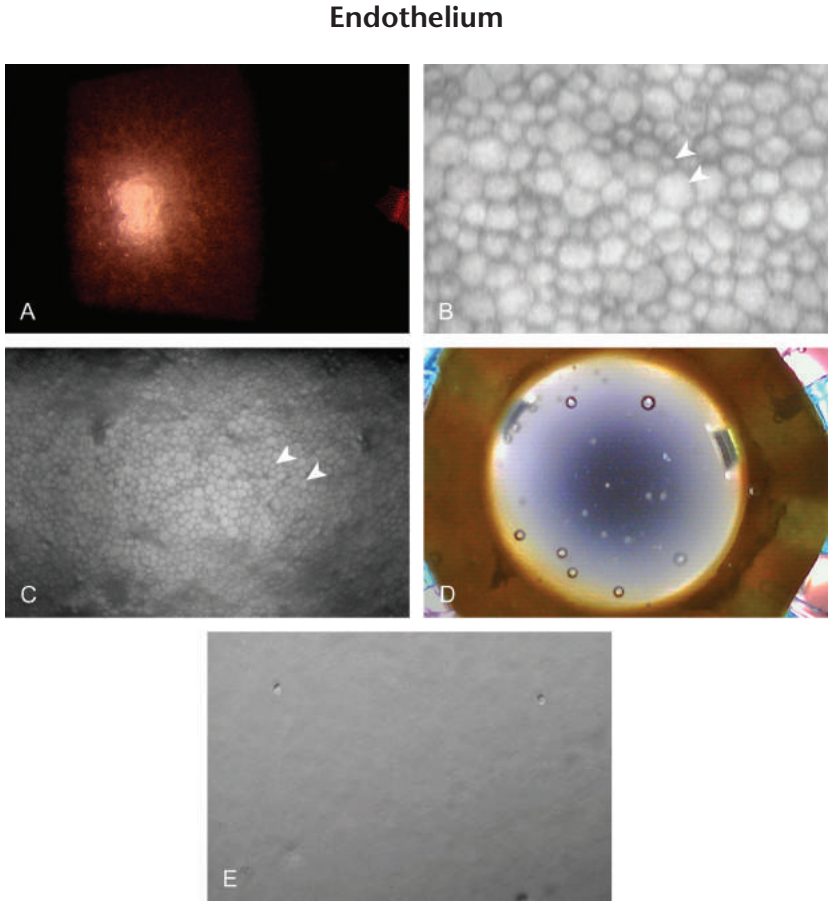

FIGURE 17. Endothelial polymegethism. A, Slit-lamp specular reflection with clearly visible cells due to varying cell sizes. B, Konan EB-10 specular microscopy demonstrating varying cell sizes (arrows). C, Konan wide-field ex vivo dual imaging specular microscopy demonstrating varying cell sizes (arrows). D and E, The Finder and Enhanced modes are unremarkable even in cases of severe polymegethism, showing no abnormality in cell function or cell damage.

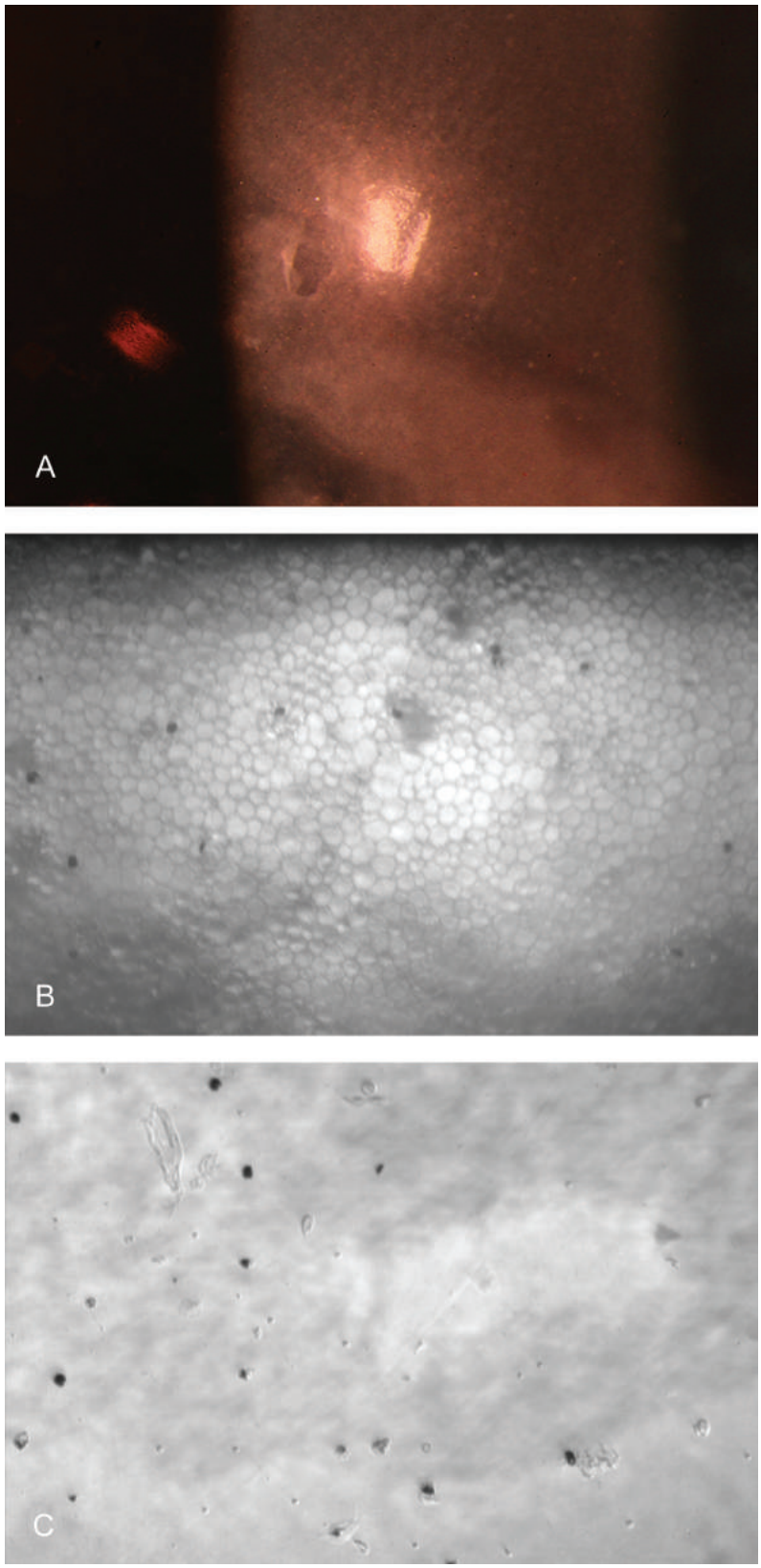

FIGURE 18. Endothelial pleomorphism. A, Slit-lamp specular reflection reveals an intact cell bed, but the cell shape is difficult to discern. B, Konan wide-field ex vivo dual imaging specular microscopy clearly demonstrates many cell shapes consistent with pleomorphism. C, The Enhanced mode shows no abnormality in cell function or cell damage.

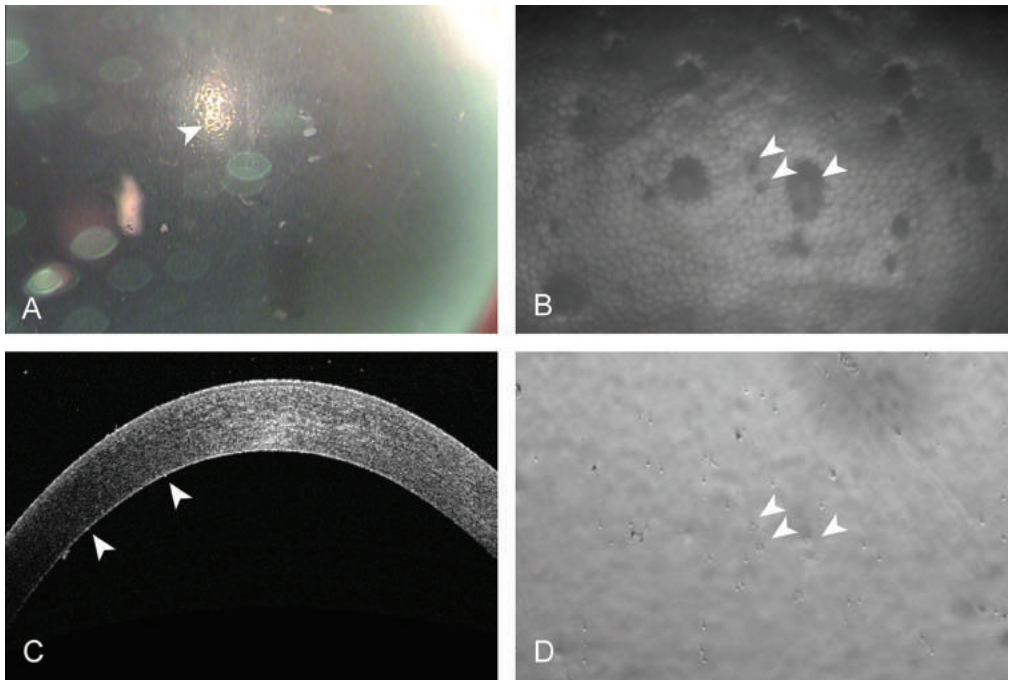

FIGURE 19. Endothelial guttae. A, Slit-lamp specular reflection shows typical "beaten metal" appearance consistent with endothelial guttae (arrow). B, Guttae are visible as dark spots on the endothelium (arrows) with Konan wide-field ex vivo dual imaging specular microscopy. C, Optical coherence tomography shows small excrescences on Descemet membrane (arrows). D, The Enhanced mode reveals the 3 dimensionality of the guttae (arrows). This is an excellent way to differentiate between cell dropout and guttae, which was difficult before the advent of this new technology.

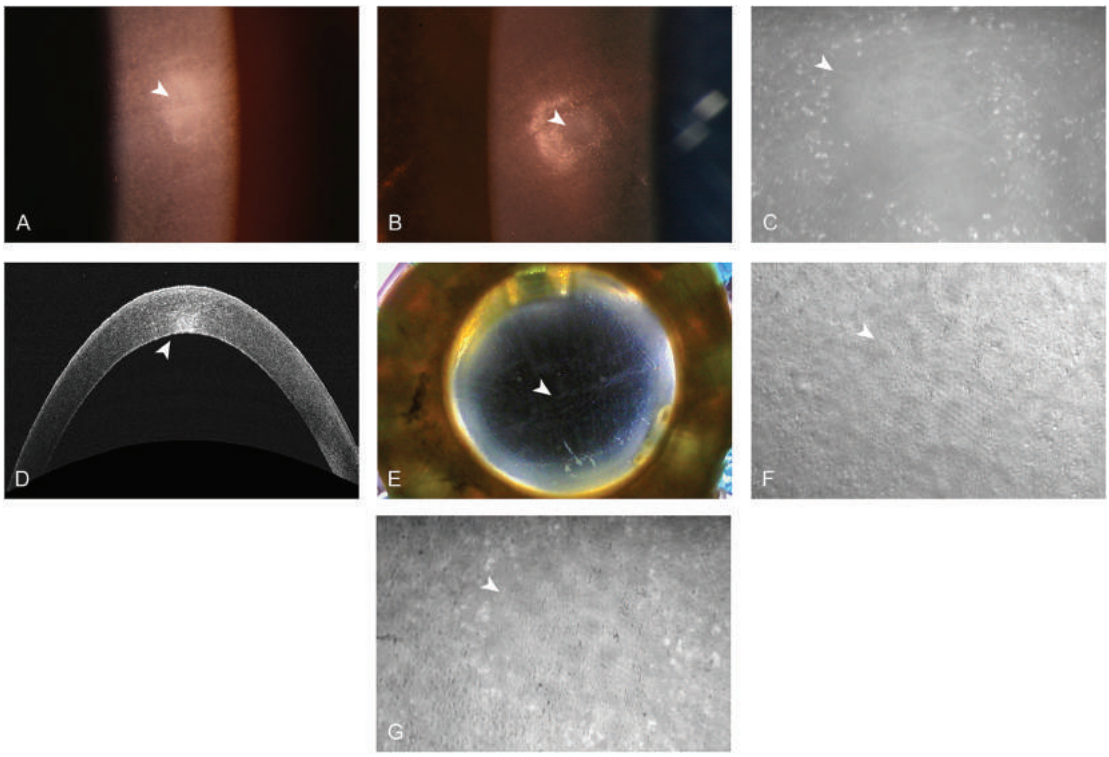

FIGURE 20. Instrument touch to the endothelium. A and B, Diffuse slit-lamp illumination demonstrates endothelial disruption within the area of specular reflection (arrows). C, Konan wide-field ex vivo dual imaging specular microscopy demonstrates a large area of nonreflectivity where cells have been denuded from Descemet membrane (arrow). D, Optical coherence tomography appears normal at the site of the defect (arrow). E, The Finder mode does not reveal any abnormality at the site of the defect (arrow). F, The Enhanced mode shows endothelial damage and areas of cell death. G, Combining enhanced and specular microscopy modes in a composite image allows for the visualization of the area of damage corresponding to cell death.

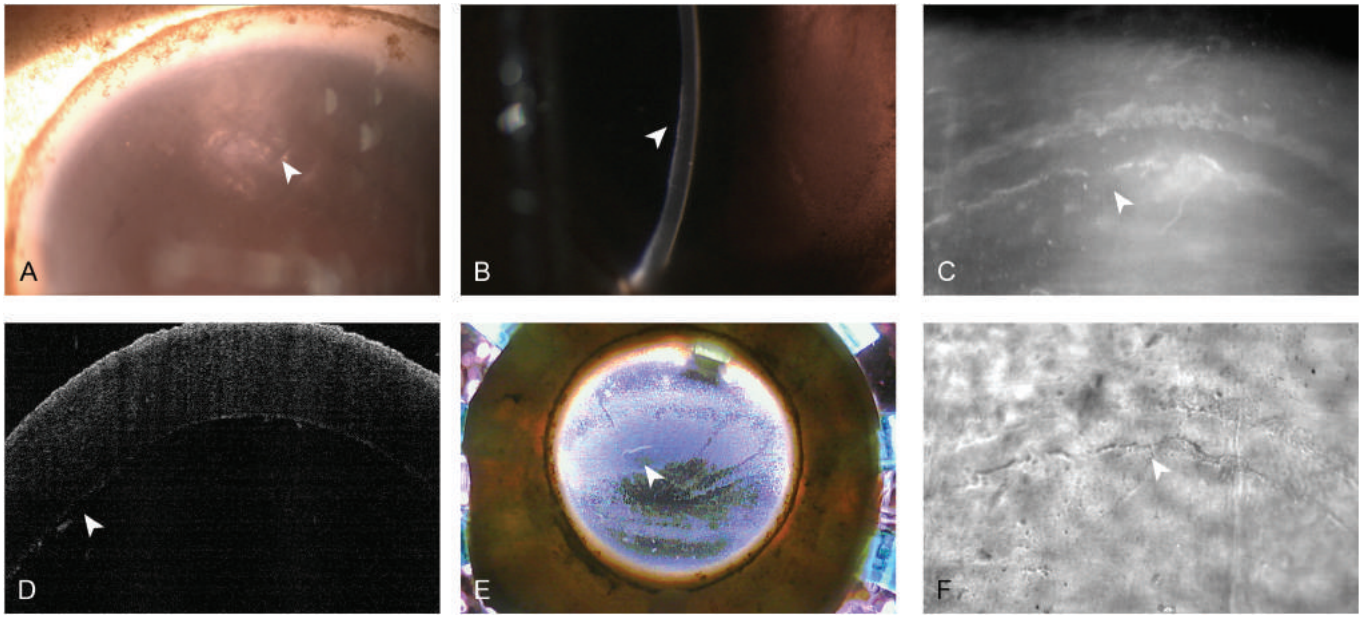

FIGURE 21. Technician-induced endothelial trauma. A and B, Endothelial damage and stromal edema are highlighted with slit-lamp illumination (arrows). C, Konan wide-field ex vivo dual imaging specular microscopy demonstrates a track of cell loss (arrow). D, Optical coherence tomography shows Descemet disruption (arrow). E, The Finder mode allows for orientation of imaging in a given area but does not reveal any abnormal pathology at the site of the defect (arrow). F, The Enhanced mode allows for visualization of cell loss at high magnification. A linear strip of cells has been denuded from overlying Descemet membrane. The interface between cells and no cells is clearly visualized (arrow).

Surgical

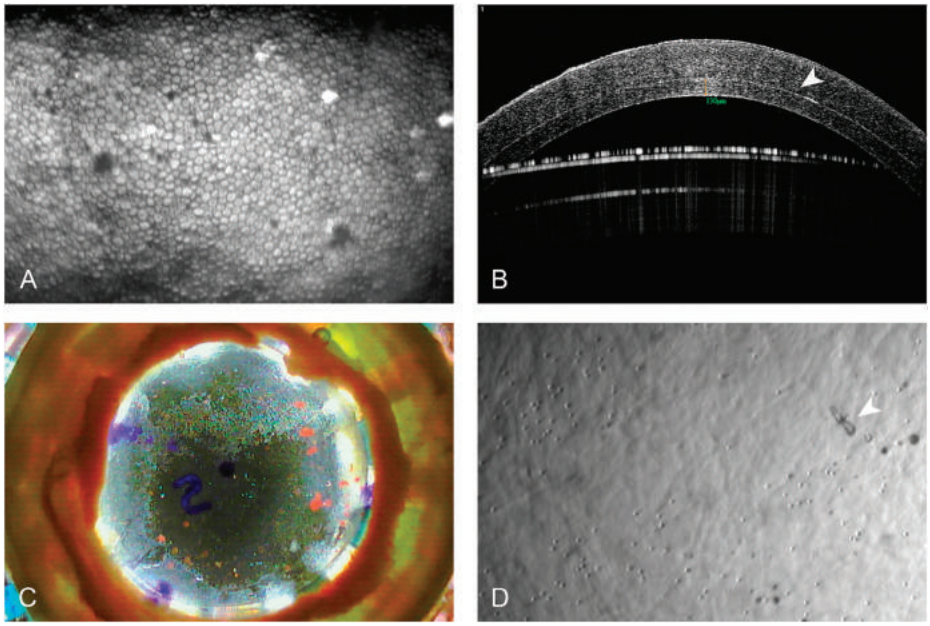

FIGURE 22. Appearance of the donor cornea after lamellar dissection for Descemet stripping automated endothelial keratoplasty (DSAEK). A, Konan wide-field ex vivo dual imaging specular microscopy showing a normal endothelial mosaic after lamellar dissection for surgery. B, Optical coherence tomography shows the stromal interface created with microkeratome dissection (arrow) and measurement of the resulting graft bed in millimeters. C, The Finder mode shows the prepared graft. Orientation marks have been added to the cornea to aid the surgeon (purple markings). D, The Enhanced mode shows the interface of the DSAEK lamellar dissection with minimal damage to endothelial cells in the process. The debris noted (arrow) allows for the user to determine pachymetry of the cut and to know that the user is at the interface.

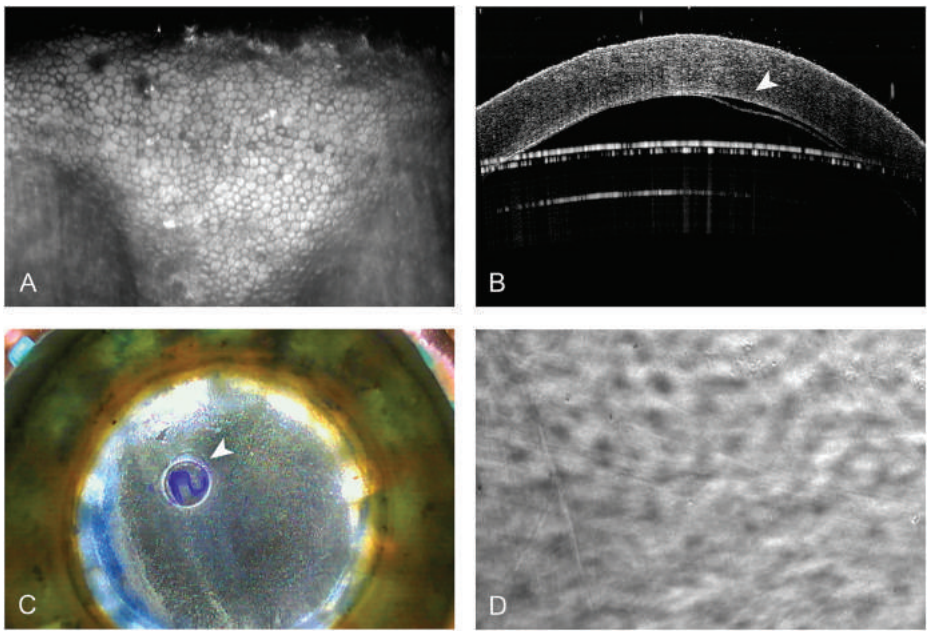

FIGURE 23. Appearance of the donor cornea after Descemet/endothelium stripping for Descemet membrane endothelial keratoplasty (DMEK). A, Konan wide-field ex vivo dual imaging specular microscopy shows an undulating mosaic of endothelial cells after Descemet membrane has been separated from overlying stroma. B, Optical coherence tomography shows that the membrane has been separated from stroma (arrow). C, The Finder mode allows for visualization of the S-stamp orientation marking and the graft edge (arrow). D, The Enhanced mode shows the interface of the DMEK peel with minimal damage to endothelial cells in the process.

EFFECTS OF WARMING

For the best quality specular image and accurate morphometric data hypothermically-stored corneas should be warmed prior to imaging and analysis.[1] Currently, tissues are warmed by either leaving tissue out at room temperature (RT) for 2–3 hours, or by using an incubator to rapidly warm the tissue (IW, incubator warming). Tissue incubation has been shown to produce better images more efficiently than corneas warmed at room temperature, and without increasing pathogen growth or increasing endothelial cell loss.[2]

Slit Lamp

The slit lamp images for both the RT and IW tissue show definite reflectivity, but poor cell definition at T0. After one hour of warming, T1, a significant improvement can be observed, and there is minimal difference between the RT and IW images, both show a bright, well defined mosaic. T2 images are essentially the same for both tissues, but at T3 the RT image quality declines slightly, which is also observed in the corresponding specular image.

Enhanced Mode

The enhanced image of both corneas at all time points is remarkably similar despite significant differences in the quality of the slit lamp and specular images at different time points. The Enhanced mode has the advantage of being less dependent on the warmth of the tissue and corresponding corneal edema which diminishes as the cornea warms.

This advantage is clear at T0 as opposed to specular microscopy, immediately after removal from hypothermic storage. Slight cell outlines for both tissues are observable, which indicates the tissue is cold; however, cell death can already be identified as small divots (arrows).

T1 through T3 images are of equivalent quality, although the RT tissue has more severe folding (arrows) than the incubated tissue; this is substantiated in the corresponding specular images (arrows). All enhanced images show cell death.

Specular Microscopy

No cell definition can be observed with specular microscopy immediately after removal from the refrigerator. However, there is vast improvement of both RT and IW tissue images from T0 to T1. The effect of the more rapid warming of the incubator can be observed in the T1 images. The RT warmed tissue has more edematous and poorly defined cell borders, and more severe folding as compared to the incubated tissue. Areas of cell death appear more significant or larger on specular microscopy as compared to the corresponding Enhanced images, because of specular reflection (arrows).

Folds persist in the RT warmed tissue at T2 and T3, which is most apparent in the specular images. Interestingly, the RT tissue image quality peaks after two hours of warming, and then appears to decline at the final imaging time point, T3, which is also true of the slit lamp image. The IW tissue has only trace folds at T3, and very good cell definition. The specular image quality of the IW tissue is better at all time points after warming has started than the RT tissue.

REFERENCES

1. Pham C, Hellier E, Vo M, Szczotka-Flynn L, Benetz B.A. LJ. Donor Endothelial Specular Image Quality in Optisol GS and Life4°C. *International Journal of Eye Banking*. 2013;1:1.
2. Tran KD, Clover J, Ansin A, et al. Rapid Warming of Donor Corneas Is Safe and Improves Specular Image Quality. *Cornea*. 2017;36: 581–587.

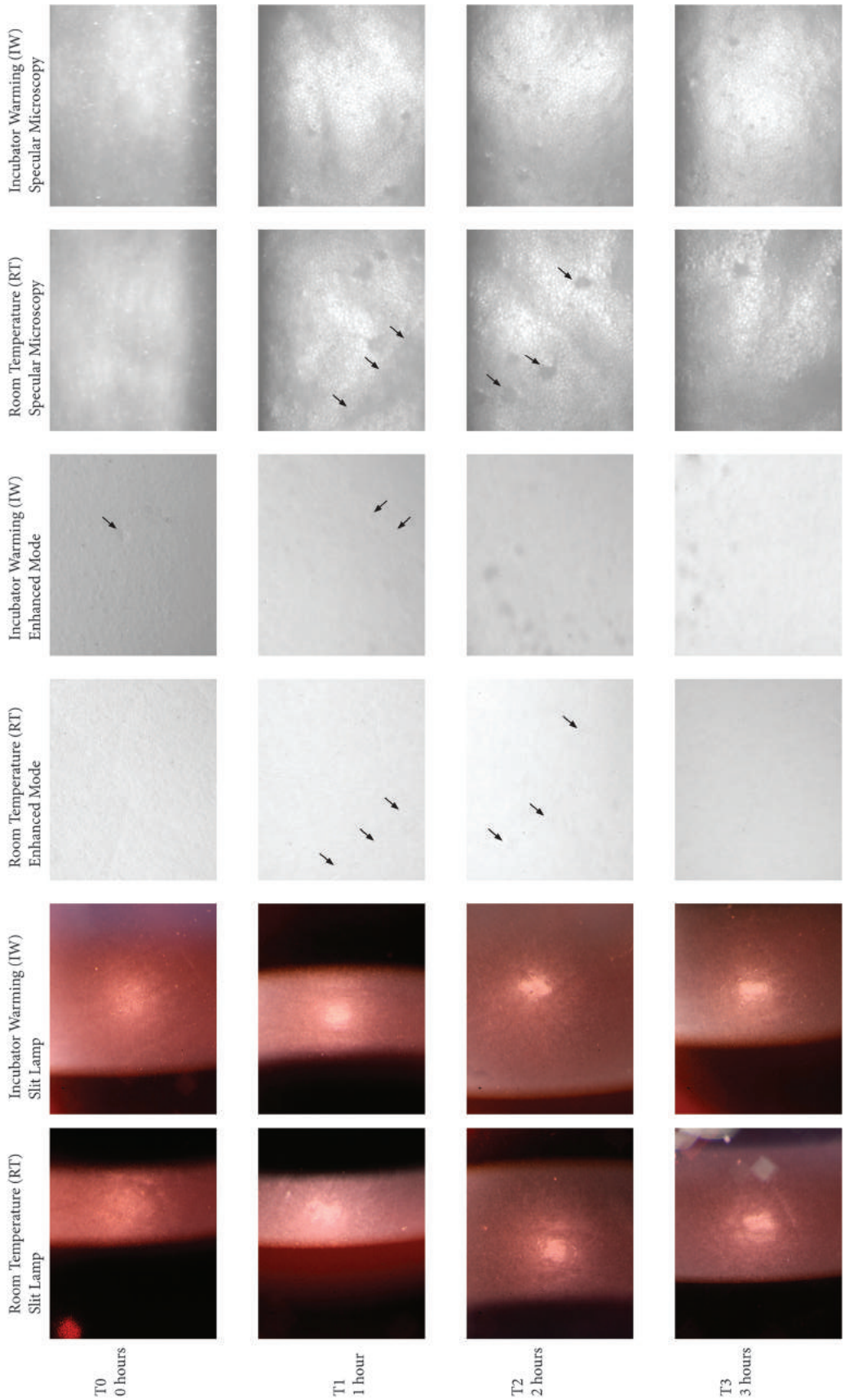

FIGURE 24. A pair of corneas was imaged by slit lamp, Enhanced mode, and specular microscopy to demonstrate the effect of incubator warming at 35°C (IW) versus sitting out at room temperature (RT) over a three hour period. The first time point was immediately after removal from hypothermic storage, and the subsequent images were taken at one hour intervals. The enhanced images are taken from the exact same location on the tissue as the specular image for the respective tissue and time point.

Other Interesting Findings

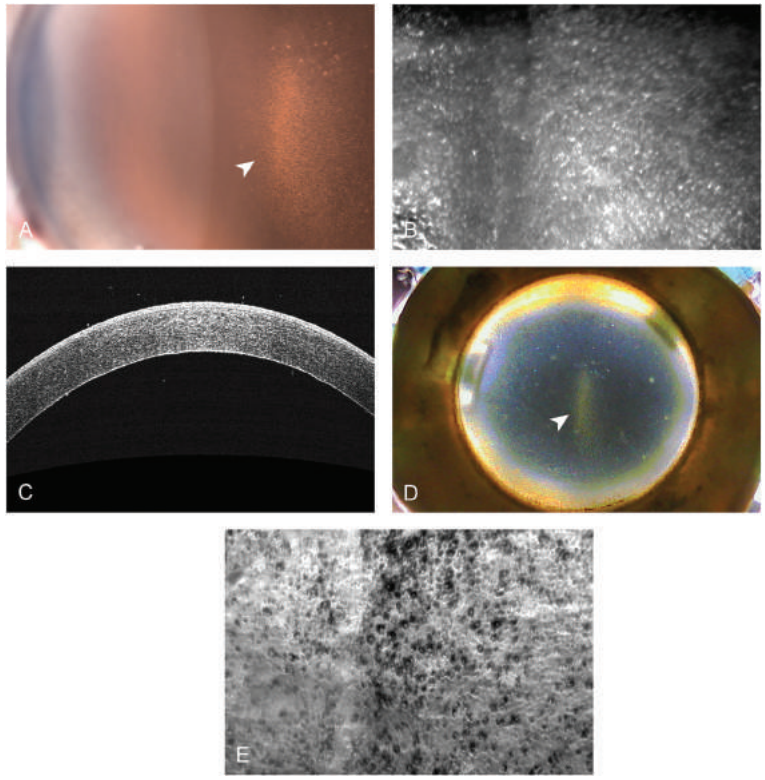

FIGURE 25. Krukenberg spindle. A, Indirect slit-lamp illumination reveals the characteristic speckled pattern of accumulated pigmented cells on the central endothelium (arrow). B, Konan wide-field ex vivo dual imaging specular microscopy shows speckled appearance obscuring views of endothelial cells. C, Optical coherence tomography appears within normal limits not having sufficient resolution to visualize endothelial deposits. D, The Finder mode shows accumulation of pigmented cells in the central cornea (arrow). E, The Enhanced mode demonstrates pigmented cells deposited on the endothelium.

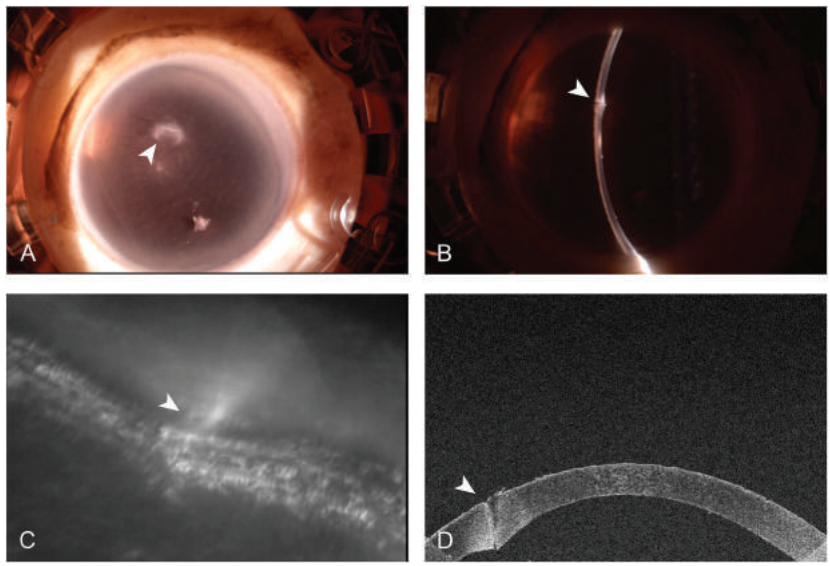

FIGURE 26. Vitreous aspiration by the medical examiner. A, Diffuse slit-lamp illumination reveals pericentral corneal opacity (arrow). B, The fine slit beam elucidates perforation of the cornea (arrow). C, HAI specular image of corneal perforation with endothelial damage adjacent to the perforation site (arrow). D, Optical coherence tomography showing a cross section of corneal perforation (arrow). The medical examiner's aspiration needle has penetrated the full thickness of the cornea.

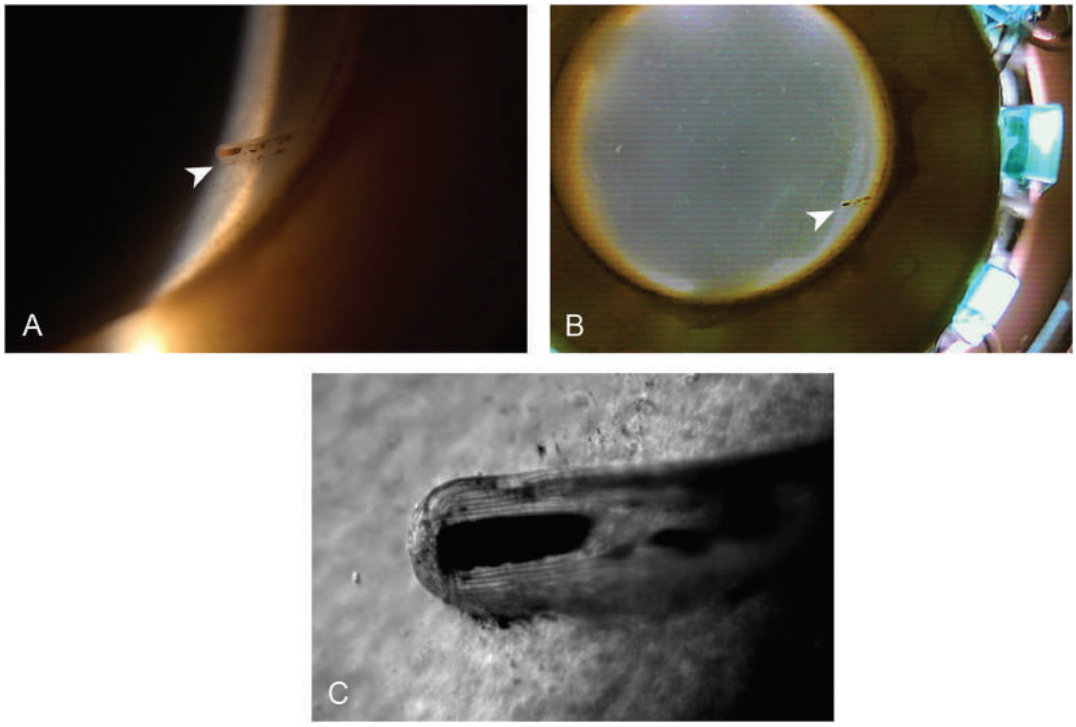

FIGURE 27. Glaucoma tube shunt. A, Diffusely illuminated slit-lamp view of a glaucoma tube shunt in the angle extending into the anterior chamber (arrow). B, The Finder mode orients the location of the glaucoma tube shunt (arrow). C, The Enhanced mode allows for high magnification of the shunt.

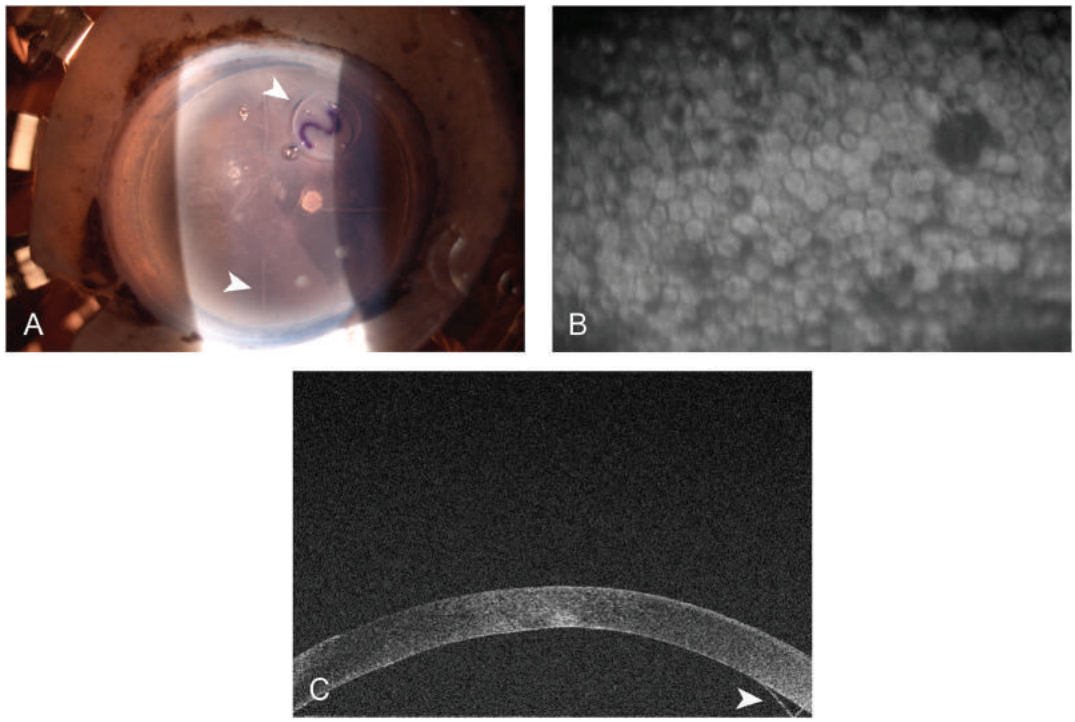

FIGURE 28. Descemet membrane endothelial keratoplasty (DMEK) preparation in a radial keratotomy donor cornea. A, S-stamp orientation mark (arrow) and radial keratotomy scars in a cornea prepared for DMEK (arrow). B, HAI specular microscopy image of the endothelium after separation of Descemet membrane from overlying stroma. C, Optical coherence tomography showing the endothelium/Descemet membrane complex has been separated from stroma (arrow) and laid back into its normal anatomic position to aid postpreparation evaluation.

Acknowledgment for Support

The coeditors and contributors are most appreciative of the financial support of staff time and funds from the following eye banks:

Cleveland Eye Bank Foundation
Eversight
Indiana Lions Eye Bank
Iowa Lions Eye Bank
Keralink
Lions VisionGift
OneLegacy
Rocky Mountain Lions Eye Bank
SightLife